A morphological analysis of thalamocortical axon fibers of rat posterior thalamic nuclei: a single neuron tracing study with viral vectors.

AUTHOR(S):

Ohno, Sachi; Kuramoto, Eriko; Furuta, Takahiro; Hioki, Hiroyuki; Tanaka, Yasuhiro R; Fujiyama, Fumino; Sonomura, Takahiro; Uemura, Masanori; Sugiyama, Kazuna; Kaneko, Takeshi

CITATION:

Ohno, Sachi ...[et al]. A morphological analysis of thalamocortical axon fibers of rat posterior thalamic nuclei: a single neuron tracing study with viral vectors.. Cerebral cortex 2011, 22(12): 2840-2857

ISSUE DATE:

2011-12

URL:

http://hdl.handle.net/2433/172452

Title

A Morphological Analysis of Thalamocortical Axon Fibers of Rat Posterior Thalamic Nuclei: A Single Neuron Tracing Study with Viral Vectors.

Sachi Ohno[1,2], Eriko Kuramoto[1], Takahiro Furuta[1], Hiroyuki Hioki[1], Yasuhiro Tanaka[1], Fumino Fujiyama[1,4], Takahiro Sonomura[3], Masanori Uemura[3], Kazuna Sugiyama[2], and Takeshi Kaneko[1]

[1]Department of Morphological Brain Science, Graduate School of Medicine, Kyoto University, Kyoto 606-8501, Japan

[2]Departments of Dental Anesthesiology and [3]Anatomy for Oral Sciences, Graduate School of Medical and Dental Sciences, Kagoshima University, Kagoshima 890-8544, Japan

[4]Core Research for Evolutionary Science and Technology, Japan Science and Technology Agency, Kawaguchi 332-0012, Japan

Running title: Single neuron tracing of thalamocortical neurons in rat posterior complex

Correspondence to: Prof. Takeshi Kaneko
Department of Morphological Brain Science
Graduate School of Medicine, Kyoto University
Kyoto 606-8501, JAPAN
Tel. 81(Japan)-75-753-4331, Fax. 81-75-753-4340
e-mail: kaneko@mbs.med.kyoto-u.ac.jp

Abstract

The rostral sector of the posterior thalamic nuclei (POm) is, together with the ventral posterior nuclei (VP), involved in somatosensory information processing in rodents. The POm receives inputs from the spinal cord and trigeminal nuclei, and projects to the primary somatosensory (S1) cortex and other cortical areas. Although thalamocortical axons of single VP neurons are well known to innervate layer (L) 4 of the S1 cortex with distinct columnar organization, those of POm neurons have not been elucidated yet. In the present study, we investigated complete axonal and dendritic arborizations of single POm neurons in rats by visualizing the processes with Sindbis viruses expressing membrane-targeted fluorescent protein. When we divided the POm into anterior and posterior parts according to calbindin immunoreactivity, dendrites of posterior POm neurons were wider but less numerous than those of anterior neurons. More interestingly, axon fibers of anterior POm neurons were preferentially distributed in L5 of the S1 cortex, whereas those of posterior neurons were principally spread in L1 with wider and sparser arborization than those of anterior neurons. These results suggest that the POm is functionally segregated into anterior and posterior parts, and that the two parts may play different roles in somatosensory information processing.

Keywords: calbindin immunoreactivity, primary somatosensory cortex, rostral sector of posterior thalamic nuclei, Sindbis virus.

INTRODUCTION

The primary somatosensory (S1) cortex mainly receives sensory signals through the 'lemniscal' pathway involving ventral posteromedial (VPM) and ventral posterolateral thalamic nuclei (VPL) in mammalian brain (for review, cf. Jones, 2007). In rodents, VPM neurons receive discriminative mechanosensory information from the trigeminal nuclei and mainly send dense axon fibers to layer (L) 4 of the S1 barrel field, which is topographically well organized in the way that a peripheral whisker functionally corresponds to a cortical column containing a barrel, a neuronal aggregate in L4, in a one-to-one fashion (for review, cf. Waite, 2004; Petersen, 2007). On the other hand, VPL neurons relay the mechanosensory information of the spinal cord to the forelimb (FL), hindlimb (HL) and trunk regions of the S1 cortex (for review, cf. Tracey, 2004). It is noticeably a characteristic organization to rodents that the HL region and medial portion of the FL region show the physiological and hodological properties of the primary motor (M1) cortex as well as that of the S1 cortex (Donoghue et al., 1979; Donoghue and Wise, 1982).

In addition to the VPL and VPM, the S1 cortex is known to receive the projection from many thalamic nuclei such as the ventral medial nucleus, intralaminar nuclei and posterior nuclei (PO) (for review, cf. Diamond, 1995; Jones, 2007). These nuclei, being a part of 'paralemniscal' and spino- and caudal trigemino-thalamic system, are considered to convey different somatosensory signals from the discriminative mechanosensory information, such as nociceptive signals and mechanosensory signals with a large receptive field. Since the ventral medial and intralaminar nuclei are known to broadly or non-specifically project to the cerebral cortex, the PO attracts attention as a specific paralemniscal relay station for the somatosensory information in cooperation with the lemniscal relay of the VPM and VPL. Actually, some PO neurons are known to receive information from the interpolar subnucleus of the spinal trigeminal nucleus and project mainly to L1 and superficial part of L5 of the S1 cortex in the rat brain (for review, cf. Diamond, 1995; Waite et al., 2004; Alloway, 2008; Petersen 2007; Rubio-Garrido P et al., 2009).

The PO is a heterogenous nucleus in mammalian brain, and divided into lateral, intermediate and medial subdivisions (Jones, 2007). Of the three subdivisions, only the medial subdivision,

which has been renamed the posterior medial nucleus by Jones, is intimately associated with the somatosensory system, relaying sensory information to somatosensory cortical areas. In rodent thalamic nuclei, the PO is mostly composed of the medial subdivision, and the medial subdivision is further divided into two parts, rostral (POm) and caudal sectors (POc). This set of abbreviations is adopted according to Diamond (1995), although the POm have often been used for indicating the whole medial subdivision of the PO. The POc in the present study is defined as the PO sector intercalated between the anterior pretectal and the medial geniculate nuclei as described previously (Diamond, 1995), and largely corresponds to the posterior intralaminar nucleus of LeDoux et al. (1985) and the triangular part of the PO of Paxinos and Watson (1986, 2007). The remaining rostral sector is much larger than the POc and located dorsomedially to the VPM and laterally to the central lateral, paracentral, parafascicular or ethmoid thalamic nucleus, and will be indicated by abbreviation POm in the present report.

The projection of VPM/VPL neurons to the S1 cortex has been studied morphologically at a single neuron level using the intra- or juxta-cellular labeling method (Arnold et al., 2001; Oda et al., 2004; Monconduit et al., 2006; Furuta et al., 2011). The cortical axon fibers of single VPM/VPL neurons terminate massively in the L4 barrel core of a cortical column and to a lesser extent in L5b and L6 beneath the barrel, serving the discriminative mechanosensory perception. In contrast, the cortical projection of single PO neurons has not been investigated in detail except for a few cases in recent juxtacellular labeling studies in the POc or posterior part of the POm (Deschênes et al., 1998; Gauriau and Bernard, 2004; Noseda et al., 2010). Thus, in the present study, to reveal the cortical projection of the POm at a single neuron level, we examined the thalamocortical axonal arborization of POm neurons in rat brain by the single neuron labeling method that was recently developed using Sindbis viral vectors expressing membrane-targeted green fluorescent protein (GFP) (Matsuda et al., 2009; Kuramoto et al., 2009; Fujiyama et al., 2011) or monomeric red fluorescent protein (mRFP) (Nishino et al., 2008). Previously, Arai et al. (1994) reported the distribution of calbindin D28k (CB) immunoreactivity in the rat thalamus, and showed that CB-immunopositive cell bodies are more sparsely distributed in the anterior part than in the posterior part of the POm (see Figs. 7, 8 in

Arai et al., 1994), suggesting that the POm was further divided into at least two parts with different chemical or molecular properties. We thus compared the axonal arborization of anterior POm neurons with that of posterior POm neurons. Finally, because we found a difference in axonal arborization between anterior and posterior POm neurons, the difference was confirmed by the conventional anterograde tracing method with *Phaseolus vulgaris* leucoagglutinin (PHA-L).

MATERIALS AND METHODS

Animals

Seventy-five adult male Sprague-Dawley rats, weighing 250–350 g, were used in the present study. Experiments were conducted in accordance with the guidelines of the animal care by Institute of Laboratory Animals, Graduate School of Medicine, Kyoto University. All efforts were made to minimize the suffering and number of animals used in the present study.

Injection of viral vector and anterograde tracer, and fixation of the brain

For single neuron labeling, after rats were anesthetized by intraperitoneal injection of chloral hydrate (35 mg/100 g body weight), we injected a mixture of Sindbis viral vectors into the POm of 59 rats bilaterally (2.9–4.7 mm posterior to the bregma, 1.8–3.0 mm lateral to the midline, and 4.7–6.4 mm deep from the brain surface) by pressure through a glass micropipette attached to Picospritzer II (General Valve Corporation, East Hanover, NJ). The mixture contained 1.5–3.0 x 10^2 infectious units each of palmitoylation site-attached GFP (palGFP)-expressing and pal-mRFP-expressing Sindbis viral vectors (Furuta et al., 2001; Nishino et al., 2008) in 0.3 µl of 5 mM sodium phosphate (pH 7.4)-buffered 0.9% saline (PBS) containing 0.5% bovine serum albumin (BSA). For conventional anterograde tracing, 16 rats were anesthetized as described above, and injected with 2.5% PHA-L (300105; J-OIL MILLS Inc., Tokyo, Japan) in 0.1M sodium phosphate buffer (PB; pH 7.4) electrophoretically by passing 7-sec-long, 2-µA-positive current pulses at 7-sec intervals for 30 min through a glass micropipette. The rats were sacrificed 48–52 hrs after the Sindbis virus injection, and 14 days after the PHA-L injection.

The 75 rats were anesthetized again with chloral hydrate (70 mg/100 g), and perfused transcardially with 200 ml of PBS, followed by 200 ml of 3% formaldehyde, 75%-saturated picric acid and 0.1 M Na_2HPO_4 (adjusted with NaOH to pH 7.0). The brains were then removed and post-fixed for 4 hrs at room temperature with the same fixative. After cryoprotection with 30% sucrose in PBS, the brains were cut into 40-µm-thick frontal sections on a freezing microtome, and the sections were collected serially in PBS.

Characterization of palGFP- or pal-mRFP-expressing thalamic neurons

The sections including the injection site of viral vectors were observed under epifluorescent microscope Axioplan 2 (Zeiss, Oberkochen, Germany) to detect thalamic neurons infected with the virus expressing palGFP (excitation 450–490 nm; emission 515–565 nm) or pal-mRFP (excitation 530–585 nm; emission ≥ 615 nm). All the following incubations were performed at room temperature and followed by a rinse with PBS containing 0.3% Triton X-100 (PBS-X). The sections containing palGFP- or pal-mRFP-positive thalamic neurons were incubated overnight with 1 µg/ml mouse monoclonal IgG1 to calbindin D28k (CB; C9848; Sigma, St Louis, MO) in PBS-X containing 0.12% lambda-carrageenan, 0.02% sodium azide and 1% donkey serum (PBS-XCD), and then for 4 hrs with 1µg/ml Alexa Fluor (AF) 647-conjugated anti-[mouse IgG] goat antibody (A21236; Invitrogen, Carlsbad, CA) in PBS-XCD. The fluorescent-labeled sections were observed under confocal laser-scanning microscope LSM5 PASCAL (Zeiss) with appropriate filter sets for GFP (excitation, 488 nm; emission, 505–530 nm), mRFP (excitation, 543 nm; emission, ≥ 560 nm) and AF647(excitation, 633 nm; emission, ≥ 650 nm), and the location of palGFP- or pal-mRFP-labeled neurons was examined in reference to CB immunoreactivity as described in the Results section. Subsequently, the sections containing palGFP- or pal-mRFP-labeled neurons were incubated for 2 hrs with 10 µg/ml propidium iodide (29037-76; nacalai tesque, Kyoto, Japan) or 1/200-diluted NeuroTrace 500/525 green fluorescent Nissl stain (N21480; Invitrogen), respectively, in PBS-X, and the location of the labeled neurons was re-examined in reference to Nissl-like staining.

Double staining for GFP or mRFP and VGluT2 immunoreactivity

The brain sections where only one palGFP- or pal-mRFP-infected neuron was contained in a hemisphere were processed for further immunoperoxidase staining. All the serial sections were incubated overnight with 0.5 µg/ml affinity-purified rabbit antibody to GFP (Tamamaki et al., 2000; Nakamura et al., 2008) or mRFP (Hioki et al., 2010) in PBS-XCD. After a rinse with PBS-X, the sections were incubated for 2 hrs with 10 µg/ml biotinylated anti-[rabbit IgG] goat antibody (BA-1000; Vector, Burlingame, CA) and then for 1 hr with avidin-biotinylated peroxidase complex (ABC) (1:100; Elite variety, Vector) in PBS-X. After a rinse in 0.1 M PB (pH 7.4), we applied biotinylated tyramine (BT)-glucose oxidase (GO) amplification method (Furuta et al., 2009; Kuramoto et al., 2009). The sections were incubated for 30 min in the BT-GO reaction mixture containing 1.25 µM BT, 3 µg/ml of GO (257 U/mg; 16831-14; nacalai tesque), 2 mg/ml of beta-D-glucose and 1% BSA in 0.1M PB (pH 7.4), followed by a wash with PBS. Subsequently, the sections were again incubated for 1 hr with ABC-Elite in PBS-X, and the bound peroxidase was finally developed brown by reaction for 30–60 min with 0.02% diaminobenzidine-4HCl (DAB; 347-00904, Dojindo, Kumamoto, Japan), and 0.0001% H_2O_2 in 50 mM Tris-HCl (pH 7.6). Subsequently, all these sections were incubated overnight with 1.0 µg/ml affinity-purified guinea pig antibody to vesicular glutamate transporter (VGluT) 2 (Fujiyama et al., 2001) in PBS-XCD containing 1% normal rabbit serum. After a rinse with PBS-X, the sections were incubated for 2 hrs with 10 µg/ml biotinylated anti-[guinea pig IgG] goat antibody (BA-7000, Vector) in PBS-X containing 1% normal rabbit serum and then for 1 hr with 1/100-dilulted ABC-Elite in PBS-X. Finally, red to fuchsia insoluble material was precipitated by 15-min incubation with 0.01% Tris-aminophenylmethane (TAPM; 35423-74, nacalai tesque), 0.07% *p*-cresol (09708-22, nacalai tesque) and 0.002% H_2O_2 in 50 mM Tris-HCl (pH 7.6) (Kaneko et al., 1994). All the stained sections were serially mounted onto the gelatinized glass slides and dried up. After washed in running water for 10 min to remove PBS and dried up overnight, the sections were cleared in xylene and then coverslipped. After reconstruction of palGFP- or pal-mRFP-labeled neurons, the sections were counterstained for Nissl with 0.2% cresyl violet to identify cytoarchitecture. The cytoarchitecture of the cerebral cortex and thalamic nuclei were mainly determined according to the atlas of Paxinos and Watson (2007).

Immunoperoxidase staining for PHA-L

The sections obtained from PHA-L-injected rats were incubated two overnights with 4 µg/ml rabbit antibody PHA-L antibody (AL-1801-2; E-Y Laboratories, Inc., San Mateo, CA) in PBS-XCD. After a rinse with PBS-X, the sections were incubated for 2 hrs with 10 µg/ml biotinylated anti-[rabbit IgG] goat antibody and then for 1 hr with 1/100-dilulted ABC-Elite in PBS-X. Subsequently, the bound peroxidase was finally developed brown by reaction for 30–60 min with 0.02% DAB, and 0.003% H_2O_2 in 50 mM Tris-HCl (pH 7.6). All the stained sections were serially mounted onto the gelatinized glass slides, dried up, dehydrated in an ethanol series, cleared in xylene, and finally coverslipped. After reconstruction, the sections were counterstained for Nissl with 0.2% cresyl violet to determine cytoarchitecture.

Reconstruction and morphological analysis of POm neurons

The cell body, dendrites and projecting axons of stained POm neurons in a frontal hemispheric 40-µm-thick section were automatically captured into a large color image by the 'normal mode' of digital slide scanner TOCO (CLARO, Aomori, Japan) with x10 objective lens (EC Plan-Neofluar; Zeiss; numerical aperture (NA) = 0.30). In the 'normal mode', the scanner took 11 images with different focuses at a site of the section (1412 µm x 1063 µm), selected the best focused image at each site, and fused those partially overlapping 20–63 images into a large image (84–260 Mbytes for each hemispheric section). Hence, at most 200 frontal images were obtained from a hemisphere with the spatial resolution of 1.038 µm x 1.038 µm. On the images, we traced and digitized the axon fibers with a digital pen tablet (Bamboo Tablet; Wacom, Saitama, Japan) and software CANVAS X (ACD Systems International Inc., Victoria, Canada). When the detail of the axon was unclear due to, for instance, intermingling of axon fibers, the reconstruction was supplemented by direct microscopic observation of the sections at a high magnification. The axon fibers were thereby reconstructed two-dimensionally section by section onto a frontal plane, and the digitized fibers from all the sections were superimposed in the computer. The cell bodies and dendrites were projected and reconstructed on a frontal plane under the microscope attached with conventional camera lucida apparatus, and the

reconstructed figures were captured into digital images by a conventional scanner. The fine morphological indices, such as inter-varicosity interval, were measured with an x100 objective lens (PlanApo100; NA = 1.4; Nikon, Tokyo, Japan). For statistical analysis, such as Bonferroni *post hoc* multiple comparison test following two-way analysis of variance (ANOVA) and Student's *t*-test, software GraphPad Prism 4 (Graphpad Software Inc., San Diego, CA) was used.

RESULTS

CB immunoreactivity in the POm

CB immunoreactivity in the POm was re-examined to reveal the chemical/molecular heterogeneity of the POm in rat brain (Fig. 1). As was reported before (Arai et al., 1994), the whole POm was weakly to moderately immunoreactive for CB. We further noticed that the posterior region of the POm was more immunoreactive for CB than the anterior region, although the border between them was not straightforward. Thus, according to regional CB immunoreactivity, the POm was divided into two parts: 1) anterior, weakly CB-immunopositive part, and 2) posterior, moderately CB-positive part (Fig. 1A"–E"). Although CB immunoreactivity in a region mainly reflected that in neuropil, CB immunoreactivity of neuronal cell bodies was mostly in parallel with neuropil immunoreactivity; only weakly immunoreactive cell bodies were found in the weakly CB-immunopositive POm (Fig. 1H), and moderately immunoreactive cell bodies and less frequently weakly immunoreactive ones were observed in the moderately CB-positive POm (Fig. 1G). Furthermore, intensely CB-immunoreactive cell bodies, with which CB immunoreactivity was clearly observed even in the proximal dendrites, were not found in the POm, but observed in intensely immunoreactive thalamic regions such as the paracentral nucleus (Fig. 1F).

Single neuron labeling of POm neurons

We injected an adequately diluted solution of Sindbis viral vectors into the anterior and posterior parts of the POm in the both sides of 59 rat brains. After fixation and sectioning of 118 hemispheres, we, for further processing, selected 30 hemispheres, each of which contained

only one pal-mRFP- or palGFP-expressing neurons under a fluorescent microscope. The localization of pal-mRFP- or palGFP-labeled neurons in the 30 hemispheres was then examined by Nissl-like counterstaining of NeuroTrace green or propidium iodide, respectively (Fig. 2A, B). Of 30 single-labeled neurons, only 15 were located within the POm, and the other 15 neurons were situated outside of the POm or on the border between the POm and surrounding nuclei. At the same time, the 15 POm neurons were classified into 8 anterior and 7 posterior POm neurons according to the strength of regional CB immunofluorescence (Fig. 2A'). Moreover, all the cell bodies of the seven posterior POm neurons showed moderate CB immunoreactivity (Fig. 2D, D'), whereas those of anterior neurons displayed weak immunoreactivity (Fig. 2C, C').

Subsequently, after immunoperoxidase staining with DAB, we further selected 5 neurons from the 8 anterior POm neurons and 5 neurons from the 7 posterior neurons, because the complete staining of the whole axonal arborization was obtained only in these 10 neurons. In the other 5 neurons, we observed that the axonal labeling faded away at the distal portion of their axonal arborization. Every end of axon fibers of the selected 10 neurons was very clearly recognized by the terminal varicosity formation of the thin axon fibers (see Fig. 4D). The location of the finally selected 10 neurons was plotted in Figure 1A"–E", and appeared dispersed within the POm except its rostralmost part (cf. injection site 123L of Fig. 8A).

Cell bodies and dendrites of POm neurons

The somal size of the POm neurons was 111–257 μm^2, and no significant difference between the anterior and posterior POm neurons was observed (Table 1). The region around each pal-mRFP- or palGFP-labeled neuron was often darkly immunostained with DAB (Fig. 2B') probably because of extracellularly leaked pal-mRFP or palGFP, suggesting an extremely strong expression of the protein by the subgenomic promoter of Sindbis viral vector. Because this immunoperoxidase staining sometimes made it difficult to measure the size of the cell body, we measured the somal size in the fluorescence images (Fig. 2C',D').

The dendrites of the 10 POm neurons were presented in Figure 3A and B. Since we noticed the difference in dendritic arborization between the anterior and posterior POm neurons, we

measured the dendritic spread (Table 1), and performed the Sholl analysis (Fig. 3C; Sholl, 1953) using the projected figures to a frontal plane. Only the mediolateral spread showed a statistically significant difference between the two POm groups (Table 1); the dendrites of posterior POm neurons more widely spread in the mediolateral direction than those of anterior POm neurons. In the Sholl analysis, we further observed that the dendrites of anterior POm neurons were more numerous than those of posterior neurons with a statistical significance at the distances of 20–100 μm from the cell body. These results support that POm neurons were segregated into anterior and posterior neurons, which were defined by the difference in regional CB immunoreactivity.

Axonal arborization of POm neurons

The axon fibers of the 10 reconstructed POm neurons were clearly labeled brown up to the end of fibers (Fig. 4B) with relatively distinct varicosities (arrowheads in Fig. 4C–E). No POm neurons reconstructed emitted axon collaterals within the POm, but all the neurons projected axon collaterals to the thalamic reticular nucleus (Fig. 4F) when the axons left the thalamic nuclei. Two of the 5 anterior POm neurons and all the 5 posterior POm neurons sent axon collaterals to the striatum (Fig. 4G; Table 2). This occurrence of striatal projection was significantly different between the two groups ($p < 0.05$ by the χ^2-test), although the difference in striatal axonal length was not significant by the two-sided unpaired *t*-test (Table 2).

The axonal arborization of the 10 single POm neurons was reconstructed up to the end of the axon fibers in Figures 5–7 and in Supplementary Figure 1. In the figures, all the subregions of the S1 cortex, such as FL, HL, head, trunk and dysgranular regions, were determined on the basis of the cytoarchitecture with the aid of VGluT2 immunoreactivity and in reference to the atlas of Paxinos and Watson (2007), Chapin and Lin (1984) and Welker et al. (1984). In the cerebral cortex, all the reconstructed POm neurons sent numerous axon fibers to the S1 cortex including the FL and HL cortices (38–94% of total axon length; Table 2, original data in Supplementary Table 1). The spread of the axonal bush in the tangential direction to the cortical surface of the S1 cortex was 1 mm and over, indicating that the spatial resolution of the POm afferents was not restricted to a barrel/column of the S1 cortex. Furthermore, all the 10

POm neurons formed another axonal arborization in the primary motor (M1), secondary motor (M2), secondary somatosensory (S2), insular, auditory or ectorhinal cortices. Fabri and Burton (1991) reported that the anteromedial part of the PO, which was included in the POm of the present study, was topographically organized in the S1 cortex. The present results were mostly in accordance with this report: 1) Neurons 1, 3, 4 and 6, which were located dorsally in the POm, projected to the HL cortex; 2) Neuron 5 and 7, being located ventrally, sent axon fibers to the S1 head region; and 3) Neuron 2 located between them projected to the FL cortex. However, in the more posterior part of the POm, the axon fibers of neurons 8, 9 and 10 were more widely distributed without clear somatotopic relationship.

In the figures of the reconstructed neurons (Figs. 5–7, Supplementary Fig. 1), it was noticed that anterior POm neurons 1–5 formed denser axonal bushes within narrower cortical regions than posterior POm neurons 6–10. It was more interesting that posterior POm neurons sent more axon fibers to L1 than anterior neurons in the S1 cortex (Table 2). In contrast, although the difference was not statistically significant, the anterior neurons sent more axon fibers to L5 in the S1 cortex than the posterior neurons (Table 2). These axon fibers in L5 were concentrated in its superficial part as reported in the previous study with the conventional anterograde tracers (Herkenham, 1980; Lu and Lin, 1993).

Koralek et al. (1988) and Chmielowska et al. (1989) reported that, in L4 of the S1 barrel cortex, the projection fibers from the POm did not terminate within the barrels, but they preferentially ended in the septal regions between barrels and in the dysgranular regions. Thus, we added the analysis of the reconstructed axonal arborizations in L4 of the S1 cortex by determining the septal and dysgranular regions with VGluT2 immunostaining (Fig. 4B) and Nissl counterstaining. In the S1 cortex, 0.0–59.8% (mean ± SD = 30.4 ± 20.4) of L4 varicose axon fibers of the POm neurons were observed in septal and dysgranular regions (Supplementary Table 2). No significant difference in the percentage was noticed between anterior and posterior POm neuron groups ($p = 0.170$ by the two-sided unpaired t-test), although the anterior group sent much more axon fibers (28.6 ± 19.5 mm) to L4 than the posterior group (5.0 ± 3.8 mm)

Posterior POm neurons 7–9 sent the axonal arborization massively to the S1 head region, but only sparsely innervated L4 without specific distribution in the septal regions. Of 5 anterior POm neurons, only neuron 5 sent axon fibers mainly to the head region of the S1 cortex (Fig. 5I) and some axon fibers in L2–4 appeared distributed in septal regions (Fig. 5J). In Figure 5K, where axon fibers in representative 3 serial sections in the S1 cortex (head region) were shown in association with the boundary of barrels and septa, the axon fibers in L4 preferred septal regions to barrel regions. However, even in anterior POm neuron 5, the thalamocortical axonal arborization was chiefly distributed to L5 of the S1 cortex.

Anterior POm neuron 1

The axonal arborization of anterior POm neuron 1 showed a large difference from the other 4 anterior neurons (Fig. 7). The main target layers were L2/3 in the M1 cortex and L2–4 in the HL cortex (Table 2), and the axonal arborization well overlapped with the distribution of VGluT2 immunoreactivity, which represented the whole thalamocortical innervation in those regions (Fig. 4A). After this difference was noticed, we extensively searched for any other differences between neuron 1 and neurons 2–5, and found that only neuron 1 was located within a small POm region containing many intensely VGluT2-immunoreactive varicosities (Fig. 7H, I). All the other POm neurons 2–10 examined in the present study were situated in much wider regions containing few VGluT2-immunoreactive varicosities (Fig. 7J, K). The POm was generally less immunoreactive for VGluT2 compared with the surrounding thalamic nuclei, such as the VPM, laterodorsal nucleus and parafascicular nucleus, but contained small islands with intensely VGluT2-immunoreactive varicosities (small arrows in Fig. 7A–E). Because VGluT2 is mainly utilized by the axon terminals of subcortical excitatory neurons (for review, see Kaneko and Fujiyama, 2002; Fremeau et al., 2004), this result indicates that the subcortical inputs to neuron 1 might be different from those to the other POm neurons. When neuron 1 was excluded from the present statistical analysis (Table 2), the relative axon length of anterior POm neurons in L5 of the S1 cortex (45.8 ± 6.2%) was significantly longer than that of posterior POm neurons (24.0 ± 13.0%).

PHA-L injection into the POm

To confirm the areal and laminar distribution of POm neurons at a population level, we carried out an additional experiment of conventional anterograde tracing. We injected anterograde tracer PHA-L into the various portions of the POm (Fig. 8). After the PHA-L injection was made in the POm except the rostralmost part, moderate to intense anterograde labeling was observed in the S1 cortex (Table 3; Fig. 9). When PHA-L was injected into the rostralmost part of the POm (injection 123L), anterograde labeling was weak in the S1 cortex but moderate in the M2, visual and cingulate cortices (Table 3). After injection of PHA-L into the weakly CB-positive anterior part of the POm (152R and 152L; Figs .8B, 9A), labeled axon fibers were distributed densely through the middle layers (L2–5), especially in the superficial part of L5, of the FL or S1 head region (Fig. 9B–D; Table 3). In L4 of both the cases, many labeled fibers were distributed in the dysgranular/septal regions of the S1 cortex. In contrast, when the injection site was located in the moderately CB-positive posterior POm (97L; Figs. 8E, 9I), labeled axon fibers were concentrated in L1 of the S1 cortex (Fig. 9J–L). This preference for L1 was also observed in cases of 91R and 133L with the injection site in the posterior POm (Table 3). Furthermore, when the injection was made on the border between the anterior and posterior parts of the POm (99R, 124L; Figs. 8C, D, 9E), many labeled axon fibers were found in both L1 and L5 of the S1 cortex (Fig. 9F–H; Table 3). Thus, these results mostly supported the present results of the single neuron tracing study.

Estimated number of varicosities in cortical axons

As axon varicosities were essential sites for synaptic transmission, it was important to estimate the number of axon varicosities of POm neurons in each layer and area. Although we tried to estimate the number of varicosities using single neuron samples, it was difficult to count the varicosities, especially those in L1, without an appropriate band-path filter as used in Figure 4C. This is mainly because dense red VGluT2 immunolabeling in L1 made it difficult to precisely detect dense brown axon varicosities (Fig. 4B). Thus, we measured the mean density of axon varicosities along the varicose axon fibers using the sections of the PHA-L tracing study (Supplementary Table 3). In those sections, axon varicosities were counted when the size of

the varicosities was more than 1.5-fold larger than the thickness of the inter-varicose fibers, and the mean density was determined area by area and layer by layer (Supplementary Table 3).

In Figure 10A, the estimated number of axon varicosities of the 10 single-labeled POm neurons were compared area by area and layer by layer. This figure shows that the S1 cortex was the largest projection target in 4 of 5 anterior POm neurons and 4 of 5 posterior POm neurons. In the S1 cortex, 6.1–38.5% (mean ± S.D. = 20.6 ± 14.6%) of axon varicosities of anterior POm neurons 2–5 were distributed in L1, whereas 40.0–91.7% (64.1 ± 19.4%) of varicosities of posterior POm neurons 6–10 were in L1. This difference was highly significant with $p = 0.008$ by the two-sided unpaired *t*-test. In contrast, anterior POm neurons 2–5 sent 40.8–54.4% (48.2 ± 6.4%) of axon varicosities to L5, and the posterior neurons projected 3.9–38.9% (24.7 ± 13.6%) of varicosities to L5 in the S1 cortex. This difference was also significant with $p = 0.016$. As was described before, all the 10 reconstructed neurons sent axon fibers outside of the S1 cortex, sometimes forming another axonal bush (Fig. 10A). When the anterior POm neurons sent axon collaterals to the M1, auditory or insular cortex, the main target layers were not L1 but L2–5. On the other hand, when the posterior POm neurons formed another axon bush in the M1, M2, S2, insular or ectorhinal cortex, the main target layer was variable; the main target layer of neurons 8 and 10 was L1, but that of neurons 6, 7 and 9 was L2–5. These findings on the axonal distribution suggest a functional difference between anterior and posterior POm neurons, and, together with the differences in CB immunoreactivity and dendritic arborization, support the segregation of the POm into the anterior and posterior parts.

DISCUSSION

In the present study, POm neurons were first divided into two groups, neurons in the weakly CB-immunopositive, anterior part and those in the moderately CB-positive, posterior part of the POm. This division was supported by the difference in axonal arborization as well as that in dendritic arborization between the two groups. Although the important cortical targets of both the anterior and posterior parts of the POm were the same S1 cortex, the axonal arborization of anterior POm neurons was less widespread and less frequent in L1, but more abundant in L5

than that of posterior neurons (Fig. 10B). This suggests a functional difference between anterior and posterior POm neurons in somatosensory information processing.

Subdivisions of the PO

Since the present study suggested the presence of two parts in the POm, the rat PO is divided into three parts in a rostrocaudal direction: the anterior POm, posterior POm and POc. The present subdivisions of the rat PO are compared with the previous partitioning by the other researchers in Table 4. Fabri and Burton (1991) divided the PO into the anteromedial and posterior parts by the presence and absence, respectively, of topographic projection to the S1 cortex. Judging from their figures, their posterior part of the PO included not only the POc but also a portion of the posterior POm. In the present study, the cortical projection of posterior POm neurons was much wider than that of anterior POm neurons, suggesting that the axons of posterior POm neurons were less topographically arranged than those of anterior neurons. Thus, the present results are compatible with the findings of Fabri and Burton (1991).

The POc of the present study was intercalated between the medial geniculate nucleus and anterior pretectal nucleus, and its main cortical target was not the S1 but the S2 cortex (Spreafico et al., 1987). We confirmed the latter property by injection of PHA-L into the POc (unpublished observation). These properties were in a good agreement with the posterior intralaminar nucleus of LeDoux et al. (1985), triangular part of the PO of Paxinos and Watson (1986, 2007), caudal sector of the PO of Diamond (1995) and posterior part of the posterior medial nucleus of Jones (2007). In addition to the caudal sector of the PO, Diamond (1995) described that the rostral sector of the PO mainly and topographically projected to the S1 cortex. This definition is compatible with the anterior POm of the present study, but not well with the posterior POm in terms of topographical projection. Thus, the posterior POm is a newly categorized portion of the PO that projected mainly and widely, thus less topographically, to L1 of the S1 cortex.

The projection of POm neurons to other cortical areas than the S1 cortex and to the striatum

Spreafico et al. (1987) reported that only a few POm neurons projected to both the S1 and S2 cortices by the double retrograde-tracing study of fluorescent dyes, and that thalamic neurons projected to the S1 and S2 cortices were largely segregated in location. In the present study, of the 10 single POm neurons labeled with the Sindbis viral vector, only 2 neurons sent axon collaterals to the S2 cortex together with main arborization to the S1 cortex. These results suggest that the same information is not so frequently relayed to both the S1 and S2 cortices simultaneously by POm neurons. However, all the single-labeled neurons in the present study projected not only to the S1 cortex but also to the other cortical areas, such as the M1/M2 (n = 7), insular (3), S2 (2), auditory (1), and ectorhinal cortices (1) (Fig. 10A,B). This fact suggests that the information transferred by POm neurons is used not only for discriminative mechanosensory perception in the S1 cortex, but also for other functions in various cortical areas.

Although no axon collaterals of VPM/VPL neurons are projected to the striatum (Deschênes et al., 1995; Oda et al., 2004; Monconduit et al., 2006; Furuta et al., 2011), 7 of the 10 single-labeled POm neurons in the present study sent axon collaterals to the striatum as was reported in rat brain (Deschênes et al., 1995). Further, there was a tendency that the POm-striatal projection was preferred by posterior POm neurons, but not by anterior POm neurons. The anterograde tracing study with PHA-L confirmed this tendency by showing that the posterior POm sent much more axon collaterals to the striatum than the anterior POm (Table 3). This result suggests a functional difference in the motor system between the anterior and posterior parts of the POm.

S1 projection of POm neurons and cortical lamination

It has been reported that the POm projects to L1 and L5 of the S1 cortex (Herkenham, 1980; Lu and Lin, 1993; Wimmer et al., 2010), which was mostly supported by the present findings except for anterior POm neuron 1. In addition, Koralek et al. (1988), Chmielowska et al. (1989) and Kichula and Huntley (2008) have reported that POm neurons send axon fibers, in L4 of the S1 cortex, to the septal/interbarrel region of the barrel field and the dysgranular region in contrast to the projection of VPM neurons to barrel cores. However, recently, Furuta et al.

(2009) showed that the septal region in L4 of the S1 cortex received selective inputs from the barreloid head, which was located in the dorsomedial region of the VPM and just beneath the border to the POm. Because the injection sites of anterograde tracers in the reports of Koralek et al. (1988) and Chmielowska et al. (1989) appeared to involve a part of the barreloid head in their figures, at least a part of anterograde labeling in L4 of the septal region or dysgranular area might be derived from the barreloid head. Furthermore, in the present study, the anterior and posterior POm neurons were shown to mainly target L5 and L1, respectively, in the S1 cortex. This is in sharp contrast to the fact that VPM neurons, including neurons in the VPM barreloid head, principally innervate L4 of the S1 cortex. Thus, the main cortical layer(s) targeted by the paralemniscal pathway via the POm is considered to differ from that by the lemniscal pathway.

Matrix/core classification of thalamic neurons and POm neurons

Recently, it has been proposed that primate and carnivore thalamic neurons are divided into core and matrix relay neurons (for review, see Jones 1998, 2001). Core neurons are found principally in primary sensory thalamic nuclei, express parvalbumin and send axon fibers to middle layers (mainly L4) of the cerebral cortex. In contrast, matrix neurons are distributed throughout the thalamic nuclei, produce CB and project preferentially to the superficial layer (L1) of the cortex. In rodent brain, however, because no relay neurons produce parvalbumin, it is difficult to differentiate thalamic neurons only by their chemical or molecular characteristics. Instead, the morphological analysis of cortical axonal arborization helped us classify the thalamic neurons to core- and matrix-like neurons. Recently, we reported that neurons in the inhibitory input-dominant zone (IZ) of the ventral anterior-ventral lateral thalamic complex (VA-VL) were mostly immunopositive for CB but negative for parvalbumin, and that IZ neurons sent 54% of axon fibers to L1 of the motor cortices (Kuramoto et al., 2009). In contrast, neurons in the excitatory subcortical input-dominant zone (EZ) of the VA-VL were negative for CB and parvalbumin, and projected 93% of axon fibers to L2–5. These findings suggest that IZ neurons are matrix neurons, whereas EZ neurons are core-like neurons.

In the present study, all the single-labeled neurons were immunopositive for CB, although neurons in the anterior POm were less immunoreactive for CB than those in the posterior POm,

suggesting that all POm neurons would be classified into matrix neurons according to Jones (1998, 2001). In addition, all the posterior POm neurons sent a substantial amount of axonal arborization to L1 of the S1 cortex, thus fulfilling the criteria for matrix neurons. In contrast, since the major target layer of anterior POm neurons 2–5 was not L1 but L5 in the S1 cortex, they were not classified to matrix neurons. This result suggests that some thalamic neurons, specifically those in the anterior POm, are neither categorized to matrix type nor to core type.

Functional consideration on POm neurons

A number of previous studies have revealed the major intrinsic connections in association with the input/output organization in the rodent S1 cortex, which includes HL and FL cortices, as follows: 1) L4 spiny neurons receive inputs from the VPM/VPL (for review, cf. Waite, 2004) and send information principally to L2/3 pyramidal neurons (Shepherd and Svoboda, 2005; Hooks et al., 2011); 2) L2/3 pyramidal neurons project axons to L5 pyramidal neurons within the S1 cortex (Kaneko et al., 2000; Cho et al., 2004; Hooks et al., 2011), or to other cortical areas; 3) L5 pyramidal neurons send the processed information to various subcortical regions, including the striatum (Mercier et al., 1990) and the POm of the thalamus (Bourassa et al., 1995; Veinante et al., 2000; Killackey and Sherman, 2003); and 4) L6 pyramidal neurons send axon fibers mainly to the VPM/VPL (for review, cf. Waite, 2004). When the inputs from the POm observed in the present study are added to this circuitry (Fig. 10C), single anterior POm neurons send their axon fibers mainly to the superficial part of L5 (L5a) of a relatively restricted region of the S1 cortex, and the main target of these axon fibers may be the basal dendrites of L5a pyramidal neurons. The presence of the latter direct synaptic connection has been revealed by the whole cell recording of L5a pyramidal neurons combined either with photo-uncaging stimulation of the POm or with optogenetic labeling of POm axons (Bureau et al., 2006; Petreanu et al., 2009).

As the main subcortical target of L5a pyramidal neurons is well known to be the striatum (Mercier et al., 1990), it is suggested that anterior POm neurons are involved in the motor control system. In addition, the paralemniscal system including the POm has recently been suggested to participate in the processing of sensor motion signals, including the frequency/rate

coding of whisker movement (Ahissar et al., 2000; Sosnik et al., 2001; Derdikman et al., 2006; Yu et al., 2006), and the POm has been shown to transmit the paralemniscal information to the S1 cortex in a manner dependent on the activity of the motor cortex (Lavallée et al., 2005; Urbain et al., 2007). It is hence conceivable that anterior POm neurons provide the cerebral cortex with sensor motion information when it is necessary for active sensing. The paralemniscal information received by L5a pyramidal neurons is in turn sent to L2 pyramidal neurons (Fig. 10C), being spread over multiple columns inside of the S1 cortex (Shepherd and Svoboda, 2005; Bureau et al., 2006). L2 pyramidal neurons also receive lemniscal information through L3 pyramidal cells, and may integrate both the lines of information from a wide region involving multiple columns (Kim and Ebner, 1999; Bureau et al., 2006).

In contrast to anterior POm neurons, the present results indicate that the main targets of posterior neurons are considered to be the apical dendrites of L2/3 and L5 pyramidal neurons. Actually, pyramidal neurons in L2/3 and L5a have been shown to receive direct synaptic inputs at their apical dendrites from the POm in a recent study (Petreanu et al., 2009). Thus, in addition to the route from anterior POm neurons to the basal dendrites of L5a pyramidal neurons, paralemniscal information might be transferred to the apical dendrites of L2/3 and L5a pyramidal neurons directly by the L1-targeting axons of posterior POm neurons. This route might constitute the second thalamocortical pathway conveying paralemniscal information. Since the L1 projection of single posterior POm neurons were highly widespread in the present study and since at least a part of the posterior POm was reported to receive noxious information (Zhang and Giesler, 2005), these thalamocortical inputs would not be helpful in the processing of fine, discriminative tactile information, but play a role in the situation that needs wide activation of the S1 cortex, such as increasing attention to the tactile inputs. To further elucidate the functional meaning for segregation of POm neurons into anterior and posterior groups, we need physiological examination based on the presence of these two groups and in conjunction with animal behavior.

Funding

This work was supported by Grants-in-Aid for Scientific Research 22300113, 22700367, 22700368, 23650175 and 23700413, and Grants-in-Aid for Scientific Research on Innovative Areas 23115101, 23123510 and 23135519 from The Ministry of Education, Culture, Sports, Science and Technology.

REFERENCES

Ahissar E, Sosnik R, Haidarliu S. 2000. Transformation from temporal to rate coding in a somatosensory thalamocortical pathway. Nature. 406:302-306.

Alloway KD. 2008. Information processing streams in rodent barrel cortex: the differential functions of barrel and septal circuits. Cereb Cortex. 18:979-989.

Arai R, Jacobowitz DM, Deura S. 1994. Distribution of calretinin, calbindin-D28k, and parvalbumin in the rat thalamus. Brain Res Bull. 33:595-614.

Arnold PB, Li CX, Waters RS. 2001. Thalamocortical arbors extend beyond single cortical barrels: an in vivo intracellular tracing study in rat. Exp Brain Res. 136:152-168.

Bourassa J, Pinault D, Deschênes M. 1995. Corticothalamic projections from the cortical barrel field to the somatosensory thalamus in rats: a single-fibre study using biocytin as an anterograde tracer. Eur J Neurosci. 7:19-30.

Bureau I, von Saint Paul F, Svoboda K. 2006. Interdigitated paralemniscal and lemniscal pathways in the mouse brain. PLoS Biol. 4:e382.

Chapin JK, Lin CS. 1984. Mapping the body representation in the SI cortex of anesthetized and awake rats. J Comp Neurol. 229:199-213.

Chmielowska J, Carvell G, Simons DJ. 1989. Spatial organization of thalamocortical and corticothalamic projection systems in the rat SmI barrel cortex. J Comp Neurol. 285:325-338.

Cho RH, Segawa S, Mizuno A, Kaneko T. 2004. Intracellularly labeled pyramidal neurons in the cortical areas projecting to the spinal cord. I. Electrophysiological properties of pyramidal neurons. Neurosci Res. 50:381-394.

Derdikman D, Yu C, Haidarliu S, Bagdasarian K, Arieli A, Ahissar E. 2006. Layer-specific touch-dependent facilitation and depression in the somatosensory cortex during active whisking. J Neurosci. 26:9538-9547.

Deschênes M, Bourassa J, Parent A. 1995. Two different types of thalamic fibers innervate the rat striatum. Brain Res. 701:288-292.

Deschênes M, Veinante P, Zhang ZW. 1998. The organization of corticothalamic projections: reciprocity versus parity. Brain Res Rev. 28:286-308.

Diamond ME. 1995. Somatosensory Thalamus of the Rat. In:Jones EG and Diamond IT, editor. Cerebral Cortex Volume 11 The Barrel Cortex of Rodents. New York (NY): Plenum Press. p 189-219.

Donoghue JP, Kerman KL, Ebner FF. 1979. Evidence for two organizational plans within the somatic sensory-motor cortex of the rat. J Comp Neurol. 183:647-664.

Donoghue JP, Wise SP. 1982. The motor cortex of the rat: cytoarchitecture and microstimulation mapping. J Comp Neurol. 212:76-88.

Fabri M, Burton H. 1991. Topography of connections between primary somatosensory cortex and posterior complex in rat: a multiple fluorescent tracer study. Brain Res. 538:351-357.

Fremeau RT Jr, Voglmaier S, Seal RP, Edwards RH. 2004. VGLUTs define subsets of excitatory neurons and suggest novel roles for glutamate. Trends Neurosci. 27:98-103.

Fujiyama F, Furuta T, Kaneko T. 2001. Immunocytochemical localization of candidates for vesicular glutamate transporters in the rat cerebral cortex. J Comp Neurol. 435:379-387.

Fujiyama F, Sohn J, Nakano T, Furuta T, Nakamura KC, Matsuda W, Kaneko T. 2011. Exclusive and common targets of neostriatofugal projections of rat striosome neurons: a single neuron tracing study using a viral vector. Eur J Neurosci. 33:668-677.

Furuta T, Tomioka R, Taki K, Nakamura K, Tamamaki N, Kaneko T. 2001. In vivo transduction of central neurons using recombinant Sindbis virus: Golgi-like labeling of dendrites and axons with membrane-targeted fluorescent proteins. J Histochem Cytochem. 49:1497-1507.

Furuta T, Kaneko T, Deschênes M. 2009. Septal neurons in barrel cortex derive their receptive field input from the lemniscal pathway. J Neurosci. 29:4089-4095.

Furuta T, Deschênes M, Kaneko T. 2011. Anisotropic distribution of thalamocortical boutons in barrels. J Neurosci. 31:6432-6439.

Gauriau C, Bernard JF. 2004. A comparative reappraisal of projections from the superficial laminae of the dorsal horn in the rat: the forebrain. J Comp Neurol. 468:24-56.

Herkenham M. 1980. Laminar organization of thalamic projections to the rat neocortex. Science. 207:532-535.

Hioki H, Nakamura H, Ma Y, Konno M, Hayakawa T, Nakamura K, Fujiyama F, Kaneko T. 2010. Vesicular glutamate transporter 3-expressing nonserotonergic projection neurons constitute a subregion in the rat midbrain raphe nuclei. J Comp Neurol. 518:668-686.

Hooks BM, Hires SA, Zhang YX, Huber D, Petreanu L, Svoboda K, Shepherd GM. 2011. Laminar analysis of excitatory local circuits in vibrissal motor and sensory cortical areas. PLoS Biol. 9:e1000572.

Jones EG. 1998. Viewpoint: The core and matrix of thalamic organization. Neuroscience. 85:331-345.

Jones EG. 2001. The thalamic matrix and thalamocortical synchrony. Trends Neurosci. 24:595-601.

Jones EG. 2007. The thalamus. 2nd ed. Cambridge (UK): Cambridge University Press.

Kaneko T, Caria MA, Asanuma H. 1994. Information processing within the motor cortex. II. Intracortical connections between neurons receiving somatosensory cortical input and motor output neurons of the cortex. J Comp Neurol. 345:172-184.

Kaneko T, Cho RH, Li YQ, Nomura S, Mizuno N. 2000. Predominant information transfer from layer III pyramidal neurons to corticospinal neurons. J Comp Neurol. 423:52-65.

Kaneko T, Fujiyama F. 2002. Complementary distribution of vesicular glutamate transporters in the central nervous system. Neurosci Res. 42:243-250.

Kim U, Ebner FF. 1999. Barrels and septa: separate circuits in rat barrel field cortex. J Comp Neurol. 408:489-505.

Killackey HP, Sherman SM. 2003. Corticothalamic projections from the rat primary somatosensory cortex. J Neurosci. 23:7381-7384.

Kichula EA, Huntley GW. 2008. Developmental and comparative aspects of posterior medial thalamocortical innervation of the barrel cortex in mice and rats. J Comp Neurol. 509:239-258.

Koralek KA, Jensen KF, Killackey HP. 1988. Evidence for two complementary patterns of thalamic input to the rat somatosensory cortex. Brain Res. 463:346-351.

Kuramoto E, Furuta T, Nakamura K, Unzai T, Hioki H, Kaneko T. 2009. Two types of thalamocortical projections from the motor thalamic nuclei of the rat: a single neuron-tracing study using viral vectors. Cereb Cortex. 19:2065-2077.

Lavalléé P, Urbain N, Dufresne C, Bokor H, Acsády L, Deschênes M. 2005. Feedforward inhibitory control of sensory information in higher-order thalamic nuclei. J Neurosci. 25:7489-7498.

LeDoux JE, Ruggiero DA, Reis DJ. 1985. Projections to the subcortical forebrain from anatomically defined regions of the medial geniculate body in the rat. J Comp Neurol. 242:182-213.

Lu SM, Lin RC. 1993. Thalamic afferents of the rat barrel cortex: a light- and electron-microscopic study using Phaseolus vulgaris leucoagglutinin as an anterograde tracer. Somatosens Mot Res. 10:1-16.

Matsuda W, Furuta T, Nakamura KC, Hioki H, Fujiyama F, Arai R, Kaneko T. 2009. Single nigrostriatal dopaminergic neurons form widely spread and highly dense axonal arborizations in the neostriatum. J Neurosci. 29:444-453.

Mercier BE, Legg CR, Glickstein M. 1990. Basal ganglia and cerebellum receive different somatosensory information in rats. Proc Natl Acad Sci U S A. 87:4388-4392.

Monconduit L, Lopez-Avila A, Molat JL, Chalus M, Villanueva L. 2006. Corticofugal output from the primary somatosensory cortex selectively modulates innocuous and noxious inputs in the rat spinothalamic system. J Neurosci. 26:8441-8450.

Nakamura KC, Kameda H, Koshimizu Y, Yanagawa Y, Kaneko T. 2008. Production and histological application of affinity-purified antibodies to heat-denatured green fluorescent protein. J Histochem Cytochem. 56:647-657.

Nishino E, Yamada R, Kuba H, Hioki H, Furuta T, Kaneko T, Ohmori H. 2008. Sound-intensity-dependent compensation for the small interaural time difference cue for sound source localization. J Neurosci. 28:7153-7164.

Noseda R, Kainz V, Jakubowski M, Gooley JJ, Saper CB, Digre K, Burstein R. 2010. A neural mechanism for exacerbation of headache by light. Nat Neurosci. 13:239-245.

Oda S, Kishi K, Yang J, Chen S, Yokofujita J, Igarashi H, Tanihata S, Kuroda M. 2004. Thalamocortical projection from the ventral posteromedial nucleus sends its collaterals to layer I of the primary somatosensory cortex in rat. Neurosci Lett. 367:394-398.

Paxinos G, Watson C. 1986. The rat brain in stereotaxic coordinates. 2nd ed. San Diego (CA): Academic Press.

Paxinos G, Watson C. 2007. The rat brain in stereotaxic coordinates. 6th ed. London (UK): Academic Press.

Petersen CC. 2007. The functional organization of the barrel cortex. Neuron. 56:339-355

Petreanu L, Mao T, Sternson S, Svoboda K. 2009. The subcellular organization of neocortical excitatory connections. Nature. 457:1142-1145.

Rubio-Garrido P, Pérez-de-Manzo F, Porrero C, Galazo MJ, Clascá F. 2009. Thalamic input to distal apical dendrites in neocortical layer 1 is massive and highly convergent. Cereb Cortex. 19:2380-2395

Shepherd GM, Svoboda K. 2005. Laminar and columnar organization of ascending excitatory projections to layer 2/3 pyramidal neurons in rat barrel cortex. J Neurosci. 25:5670-5679.

Sholl DA. 1953. Dendritic organization in the neurons of the visual and motor cortices of the cat. J Anat. 87:387-406.

Sosnik R, Haidarliu S, Ahhisar E. 2001. Temporal frequency of whisker movement. I. Representations in brain stem and thalamus. J Neurophysiol. 86:339-353.

Spreafico R, Barbaresi P, Weinberg RJ, Rustioni A. 1987. SII-projecting neurons in the rat thalamus: a single- and double-retrograde-tracing study. Somatosens Res. 4:359-375.

Tamamaki N, Nakamura K, Furuta T, Asamoto K, Kaneko T. 2000. Neurons in Golgi-stain-like images revealed by GFP-adenovirus infection in vivo. Neurosci Res. 38:231-236.

Tracey D. 2004. Somatosensory System. In: Paxinos G, editor. The rat nervous system. 3rd ed. San Diego: Elsevier. p 797-815.

Urbain N, Deschênes M. 2007. Motor cortex gates vibrissal responses in a thalamocortical projection pathway. Neuron. 56:714-725.

Veinante P, Lavalléé P, Deschênes M. 2000. Corticothalamic projections from layer 5 of the vibrissal barrel cortex in the rat. J Comp Neurol. 424:197-204.

Waite PME. 2004. Trigeminal Sensory System. In: Paxinos G, editor. The rat nervous system. 3rd ed. San Diego (CA): Elsevier. p 817-851.

Welker W, Sanderson KJ, Shambes GM. 1984. Patterns of afferent projections to transitional zones in the somatic sensorimotor cerebral cortex of albino rats. Brain Res. 292:261-267.

Wimmer VC, Bruno RM, de Kock CP, Kuner T, Sakmann B. 2010. Dimensions of a projection column and architecture of VPM and POm axons in rat vibrissal cortex. Cereb Cortex. 20:2265-2276.

Yu C, Derdikman D, Haidarliu S, Ahissar. 2006. Parallel thalamic pathways for whisking and touch signals in the rat. PLos Biol. 4:e124.

Zhang X, Giesler GJ Jr. 2005. Response characteristics of spinothalamic tract neurons that project to the posterior thalamus in rats. J Neurophysiol. 93:2552-2564.

Table 1. Soma and dendrites of single-labeled POm neurons.

	anterior POm neurons	posterior POm neurons	*p* value[1)]
Number of neurons	5	5	
Soma area [μm^2]	183 ± 25[2)]	153 ± 12	0.317
Dendritic spread			
Rostrocaudal [μm]	360 ± 28	312 ± 115	0.172
Mediolateral [μm]	329 ± 31	450 ± 29	0.022
Dorsoventral [μm]	305 ± 18	308 ± 26	0.938

1) *p* value was calculated by the two-sided unpaired *t*-test.

2) Mean ± S.D.

Table 2. Estimated axon length of single-labeled POm neurons in the cerebral cortex and striatum. For original data, see Supplementary Table 1.

Neuron number	total axon length in cortex[1)] [μm]	total axon length in S1 cortex [1)] [μm]	L1 axon length in S1 cortex [1)] [μm]	L5 axon length in S1 cortex [1)] [μm]	axon length in the striatum[1)] [μm]
anterior POm neurons					
1	242392	146639 (60.5%)[2)]	4300 (2.9%)[3)]	26762 (18.3%)[3)]	0
2	227693	87140 (38.3)	32409 (37.2)	34203 (39.3)	617
3	178957	168369 (94.1)	9593 (5.7)	70304 (41.8)	0
4	193751	147332 (76.0)	37525 (25.5)	74935 (50.9)	0
5	115024	95964 (83.4)	10736 (11.2)	49231 (51.3)	19032
1–5	191564 ± 49777[4)]	129089 ± 35499 (70.5 ± 21.8)	18913 ± 14965)** (16.5 ± 14.5**)	51087 ± 21320 (40.3 ± 13.4)	3930 ± 8447
2–5	178856 ± 47193	124701 ± 39394 (73.0 ± 24.3)	22566 ± 14479* (19.9 ± 14.2**)	57158 ± 18961 (45.8 ± 6.2*)	4912 ± 9418
posterior POm neurons					
6	236247	187629 (79.4%)	103878 (55.4%)[3)]	54567 (29.1%)[3)]	6309
7	210462	113281 (53.8)	81714 (72.1)	21642 (19.1)	615
8	209574	87569 (41.8)	50976 (58.2)	26776 (30.6)	2134
9	175332	116703 (66.6)	44858 (38.4)	43613 (37.4)	6400
10	160763	69108 (43.0)	62807 (90.9)	2641 (3.8)	6729
6–10	198476 ± 30213[4)]	114858 ± 45109 (56.9 ± 16.1)	68847 ± 24104 (63.0 ± 19.7)	29848 ± 20109 (24.0 ± 13.0)	4437 ± 1275

1) The length of axon fibers was estimated by multiplying the length of varicose axons projected onto a frontal plane by $\pi/2$. Thus, the measured axon length did not contain non-varicose thick axon fibers which was unlikely to make synaptic contacts. The S1 cortex included the FL and HL cortices in this table.

2) The relative length in the S1 cortex to the total axon length in the whole cerebral cortex.

3) The relative length in L1 or L5 to the total axon length in the S1 cortex.

4) Mean ± S.D.

**, $p < 0.01$; *, $p < 0.05$ compared between anterior and posterior POm neurons by the two-sided unpaired *t*-test.

Table 3. The summary of the distribution of anterogradely labeled axon fibers after injection of PHA-L into several regions of the POm. The axonal density was semi-quantitatively evaluated with the following internal standards using the section centered in the labeled region: +++, FL cortex in Fig. 9C; ++, S2 cortex in Fig. 9D; +, M1 cortex in Fig. 9K; –, no axon fibers.

Injection site (Fig. 8)	CB immuno-reactivity in POm	Target cortices (layers) S1[1)] (L1)	(L2–5)	S2	M1	M2	Insular	Parietal associa-tion	Audi-tory	Ecto-rhinal	Visual	Cingu-late	Striatum
123L	(+)	±	±	–	–	++	–	–	–	–	++	++	+
152R	(+)	+~++	+++	++	++	–	–	–	–	–	±	–	–
152L[2)]	(+)	+~++	+++	+~++	++	+	–	–	–	–	–	–	–
99R	border[3)]	++	++~+++	++	+~++	+~++	–	±	++~+++	–	–	–	+
124L	border	++~+++	+++	+~++	++	–	+~++	++	+	±	++	–	+
95L	(++)	++~+++	++	+	+	–	++	±	–	+	+~++	–	+
91R	(++)	+++	+	++	++	++	++~+++	–	±	+~++	–	–	++
97L	(++)	+++	+	++	++	+~++	+++	+~++	+	+~++	–	–	++
133L	border	++~+++	+	++~+++	±	±	++~+++	±	±	+	–	–	++

1) The S1 cortex included the FL and HL cortices in this table.

2) The injection site involved the border between POm and VPM, and the projection site included the S1 head regions, where septal L4 was partly innervated by the axon fibers.

3) The injection site was located on the border of CB(+) and CB(++) regions.

Table 4. Partitioning of the medial subdivision of the rat PO.

Weakly CB-positive mainly project to S1L5 topographical	Moderately CB-positive mainly project to S1L1 less topographical	Moderately CB-positive mainly project to S2 –	
Anterior part of POm	Posterior part of POm	POc	present study
(not described)	(not described)	Posterior intralaminar nucleus	LeDounx et al., 1985
Posterior nucleus	Posterior nucleus	Triangular part of PO	Paxinos and Watson, 1986
Anteromedial part of PO	Posterior part of PO?	Posterior part of PO	Fabri and Burton, 1991
Rostral sector of PO	?	Caudal sector of PO	Diamond, 1995
Anterior part of posterior medial nucleus	Anterior part of posterior medial nucleus?	Posterior part of posterior medial nucleus	Jones, 2007

Figure legends

Figure 1. CB immunoreactivity of the rat POm, and the location of the single POm neurons analyzed in the present study. Although the cytoarchitecture of the POm appeared homogeneous in the frontal sections (**A–E**), CB immunoreactivity showed some heterogeneity in the POm of subsequent sections (**A'–E'**). CB immunoreactivity was semi-quantitatively evaluated with internal standards, intense (+++) in the paracentral nucleus (Pc; **F**), moderate (++) in the posterior part of the POm (**G**), weak (+) in the anterior part of the POm (**H**), and almost negative (–) in the VPM (**I**). The distribution of CB immunoreactivity was illustrated in **A"–E"**, where moderately CB-immunoreactive regions were darkly, and weakly immunoreactive regions were lightly painted. The distributions of single-labeled POm neurons were projected onto the nearest frontal plane of **A''-E''**. APt, anterior pretectal nucleus; CL, central lateral nucleus; Eth, ethmoid nucleus; fr, fasciculus retroflexus; Hb, habenular nucleus; LD, laterodorsal nucleus; LGd, dorsal lateral geniculate nucleus; LP, lateral posterior nucleus; MD, mediodorsal nucleus; ml, medial lemniscus; Pf, parafascicular nucleus; PLi, posterior limitans nucleus; R, thalamic reticular nucleus; Sc scafoid nucleus; VM, ventral medial nucleus. Scale bar in **E''** applies to **A–E''**; that in **I** to **F–I**.

Figure 2. Identification and CB immunoreactivity of single-labeled POm neurons. When a neuron infected with pal-mRFP (**A**) or palGFP Sindbis virus was found under fluorescence microscope (arrowheads), the section containing the labeled neuron was counterstained with NeuroTrace green (NTG; **A**, **B**) or propidium iodide, respectively, for cytoarchitecture and immunostained for CB (AF647; pseudo-colored with cyan; **A'**, **C**, **D**). The neuron was classified to the anterior or posterior POm neuron according to the intensity of regional CB immunoreactivity. All the infected neurons in the anterior POm showed weak CB immunoreactivity in their cell bodies (**C**, **C'**), whereas most infected neurons in the posterior POm showed moderate CB immunoreactivity (**D**, **D'**). After the location and CB immunoreactivity of the infected neurons were examined, the infected neurons were visualized

by the immunoperoxidase staining with the anti-mRFP (**B'**) or anti-GFP antibody. Scale bar in **A'** applies to **A**, **A'**; that in **B'** to **B**, **B'**; that in **D'** to **C–D'**.

Figure 3. Dendrites and cell bodies of reconstructed POm neurons. Anterior POm neurons (1–5; **A**) had much more dendritic processes than posterior POm neurons (6–10; **B**). The Sholl analysis revealed that the difference was statistically significant at distances of 20–100 μm from the cell body (**C**; $*p < 0.05$, $***p < 0.001$, Bonferroni multiple comparison test). The open and filled circles in **C** are the averaged data for anterior and posterior POm neurons, respectively, and bars indicate S.D. Scale bar applies to **A** and **B**.

Figure 4. Axonal arborization of single-labeled POm neurons in the cerebral cortex and striatum. In the S1 cortex, the axon fibers of a POm neuron, which was immunostained brown with the anti-mRFP antibody, were distributed mainly in L1–3 and L5 (DAB; **A**, **B**). Because the sections were further immunostained red for VGluT2 (TAPM/*p*-cresol), the L4 barrel (asterisks in **B**) and septal structures (small arrows) of the S1 head region were clearly observed as reported previously (Fujiyama et al., 2001). The size and inter-varicosity interval of axon varicosities (arrowheads in **C–E**) of the POm neuron was larger and longer, respectively, in L2/3 than those in L1 and L5. In addition, every end of axon fibers was clearly visualized, usually forming a similar varicosity (double arrowhead in **D**). The neuron also sent axon collaterals to the thalamic reticular nucleus (R; **F**) and striatum (CPu; **G**). Red VGluT2 immunoreactivity in **C–G** was suppressed by using a 600-nm-centered band-path filter. Scale bar in **E** applies to **C–E**; that in **G** to **F, G**.

Figure 5. Axonal arborization of anterior POm neurons. Anterior POm neurons formed relatively dense axonal bushes in the S1 cortex including the FL and HL cortices (**A**, **D, F, I**). The axon fibers of anterior POm neurons were densely distributed in L5 of the S1 cortex (blue lines in **B**, **E, G, J**). In addition, some neurons made another axonal bush in a different cortical region, such as the M1, auditory (Au), and insular (Ins) cortices (**C**, **H**, **L**). The S1 cortex was subdivided into HL, FL, head, and dysgranular (Dys) regions. In **K**, the axonal reconstruction

of 3 serial sections was shown in association with the boundary of septa and barrels (continuous gray lines), and L4 axon fibers in the septa and barrels were indicated as continuous and broken green lines, respectively.

Figure 6. Cortical axonal arborization of posterior POm neurons. The axons of posterior POm neurons were more widespread and less densely distributed in the cerebral cortex than those of anterior POm neurons (**A**, **D, G, K**), although the bush invariably included the S1 including the FL and HL cortices (**B, F, H, I, L, M**). Furthermore, in contrast to anterior POm neurons, the axonal arborization preferred L1 to the other cortical layers (red lines in **B, C, E, F, H–J, L–O**). The S1 cortex was subdivided into HL, FL, trunk (Tr), head, and dysgranular (Dys) regions. Ect, ectorhinal cortex; Ins, insular cortex.

Figure 7. Anterior POm neuron 1. Of the 10 reconstructed neurons, neuron 1 was located at the most rostral portion of the POm (Fig. 1). This neuron sent axon fibers mainly to L2–4 of the M1 an HL cortices without projecting collaterals to the striatum (**F, G**). This is in a sharp contrast to the other POm neurons whose main target was L1 or L5 of the cerebral cortex. Of the 10 neurons, only neuron 1 was located in the regions that contained intensely VGluT2-immunoreactive varicosities (**H**, **I**) and were scattered in the POm (small arrows in **A**–**E**). The sections of **A**–**E** were the adjacent sections of those used in Figure 1A–E, A'–E'. The other POm neurons 2–10 were situated in the region containing few VGuT2-immunoreactive varicosities (**J**, **K**). Abbreviations, see the legend of Figure 1. Scale bar in **E** applies to **A**–**E**; that in **J** to **H, J**; that in **K** to **I, K**.

Figure 8. The injection sites of anterograde tracer PHA-L. Each number in the box indicates the animal number and the side of the injection site. The lines in the figures were drawn on the basis of CB immunoreactivity and cytoarchitecture in the adjacent sections as shown in Figure 1. VL, ventral lateral nucleus; for the other abbreviations, see the legend of Figure 1. Scale bar in **F** applies to **A–F**.

Figure 9. Anterograde projection of POm neurons after injections of PHA-L into the POm. Three representative results are shown here: When PHA-L was injected into the anterior part of POm (152R; **A**), labeled axon fiber were observed mainly in middle layers, L2–5, of the FL cortex and the dysgranular (Dys) regions of the S1 cortex (**B–D**). In contrast, after the injection of PHA-L into the posterior POm (97L; **I**), projected axon fibers were found widely and intensely in L1 of the M1, S1 and S2 cortices (**J–L**). When the injection was made on the border between the anterior and posterior POm (99R; **E**), the distribution of the axon fibers were intermediate between the above two cases, and the arborization was concentrated to L1 and L5 of the FL and HL cortices, and to those of the Dys region of the S1 cortex. The S1 cortex was subdivided into HL, FL, trunk (Tr), shoulder (Sh), head, and Dys regions. Au, auditory cortex; Cg, cingulate cortex; Ect, ectorhinal cortex; Ins, insular cortex; PtA, parietal association cortex. Scale bar in **I** applies to **A, E, I**; that in **L** to **B–D**, **F–H**, **J–L**.

Figure 10. Summary of the present results. **A**; The estimated number of axon varicosities of single-labeled POm neurons was calculated using the data on the axonal length of the neurons and the density of axon varicosities (Supplementary Tables 1, 3). All the reconstructed POm neurons sent a substantial amount of axon varicosities to the S1 cortex, which included the FL and HL cortices, and almost all the POm neurons distributed axon varicosities in other cortical areas. **B**; Schematic diagram of POm projections. **C**; Input/output organization and local cortical circuit in the S1 cortex. For further detail in **B** and **C**, see the text. Au, auditory cortex; Ect, ectorhinal cortex; Ins, insular cortex; R, thalamic reticular nucleus.

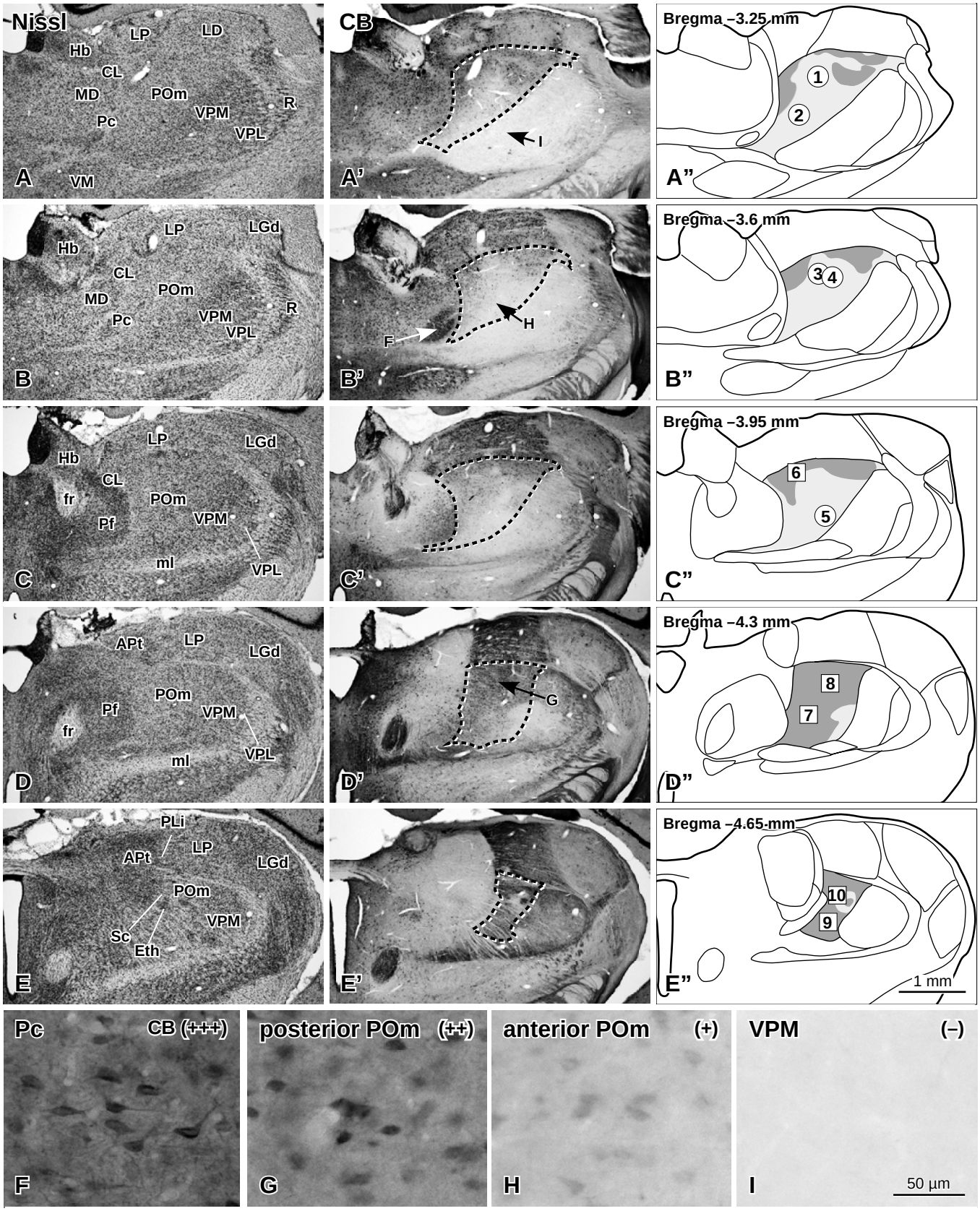

Fig. 1 Ohno et al., 178 x 223 mm (double column width) No reduction.

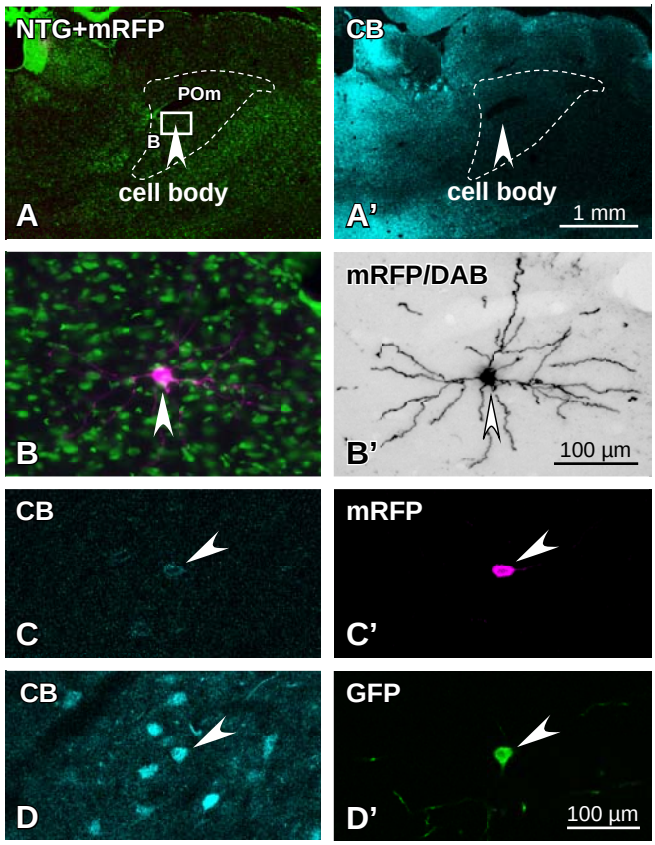

Fig. 2 Ohno et al., No reduction.
86 x 111 mm (single column width)

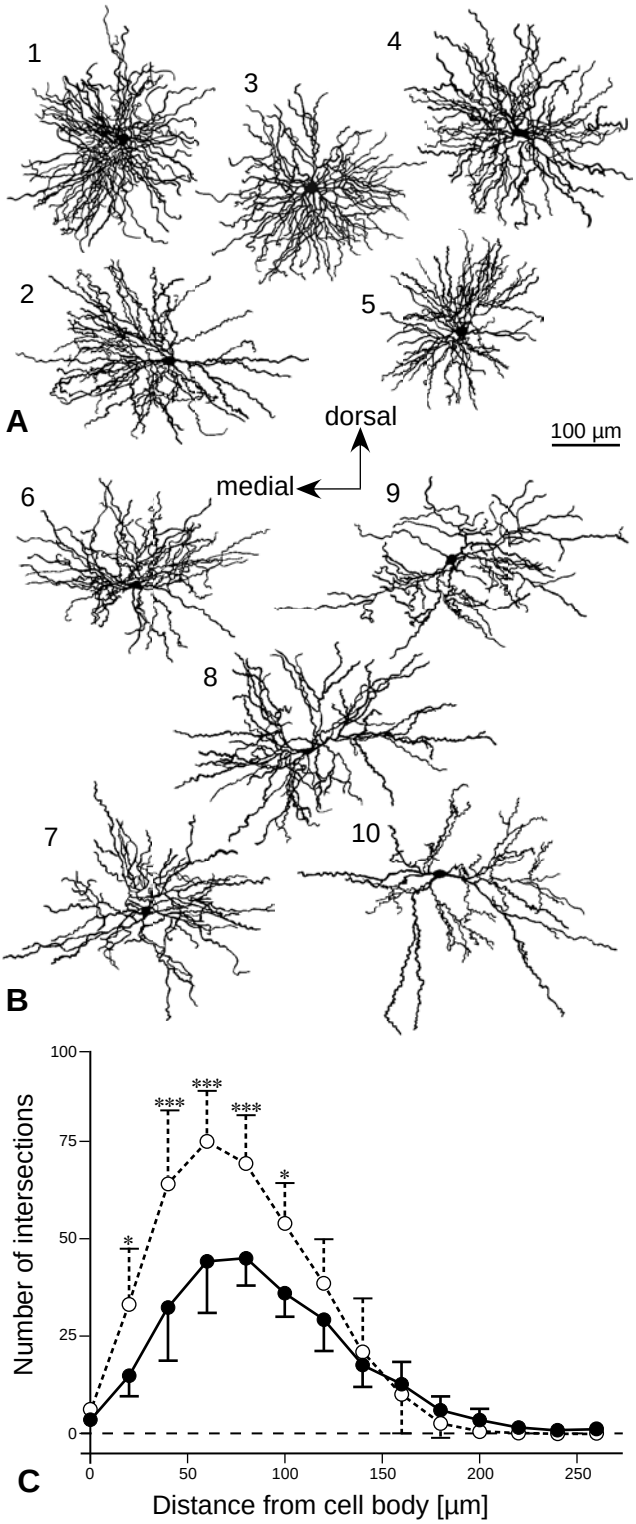

Fig. 3 Ohno et al., No reduction.
85 x 200 mm (single column width)

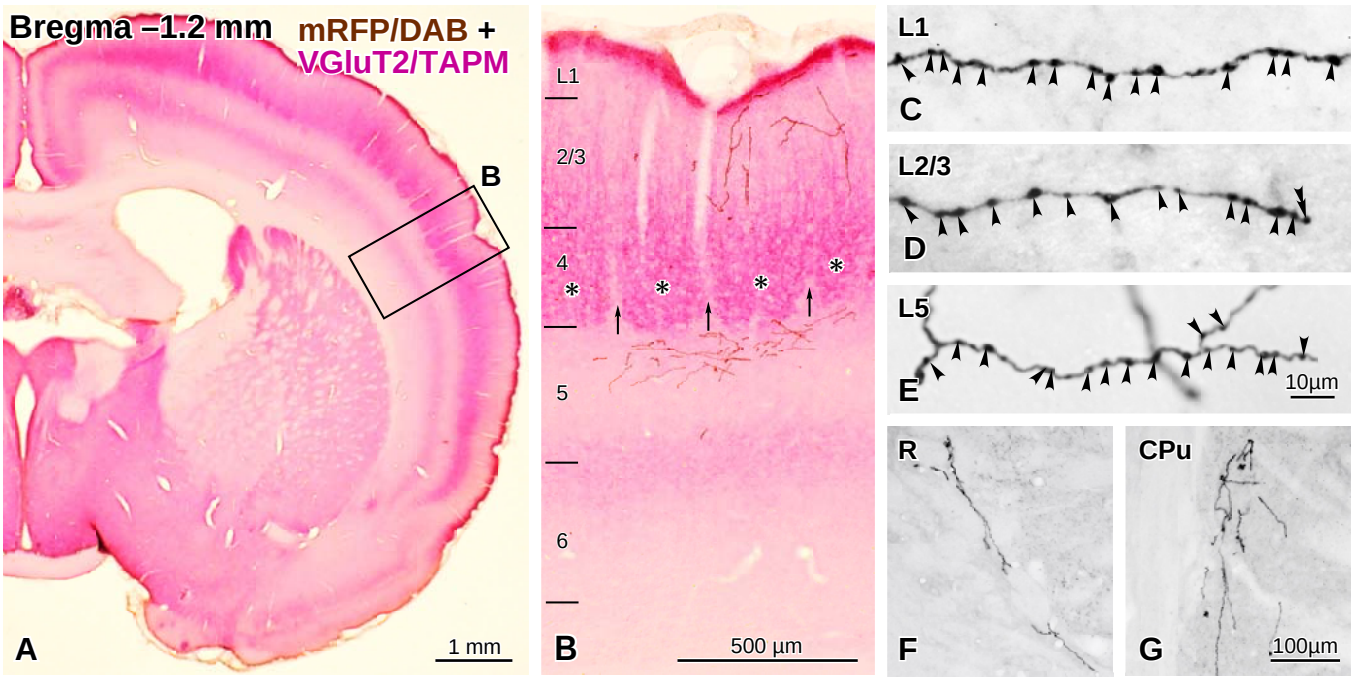

Fig. 4 Ohno et al., 179 x 90 mm (double column width) No reduction.

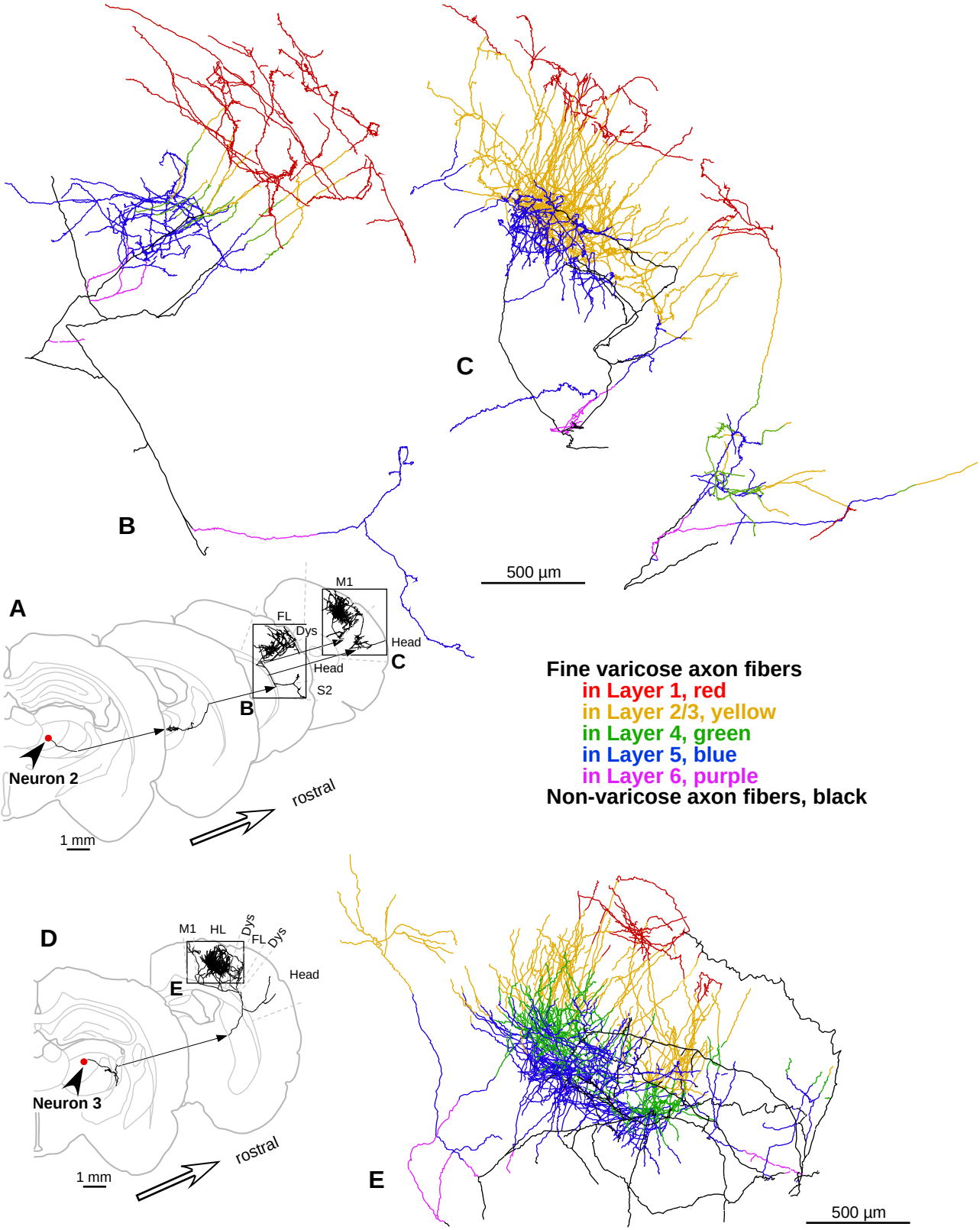

Fig. 5-1 Ohno et al., 169 x 212 mm (double column width) No reduction.

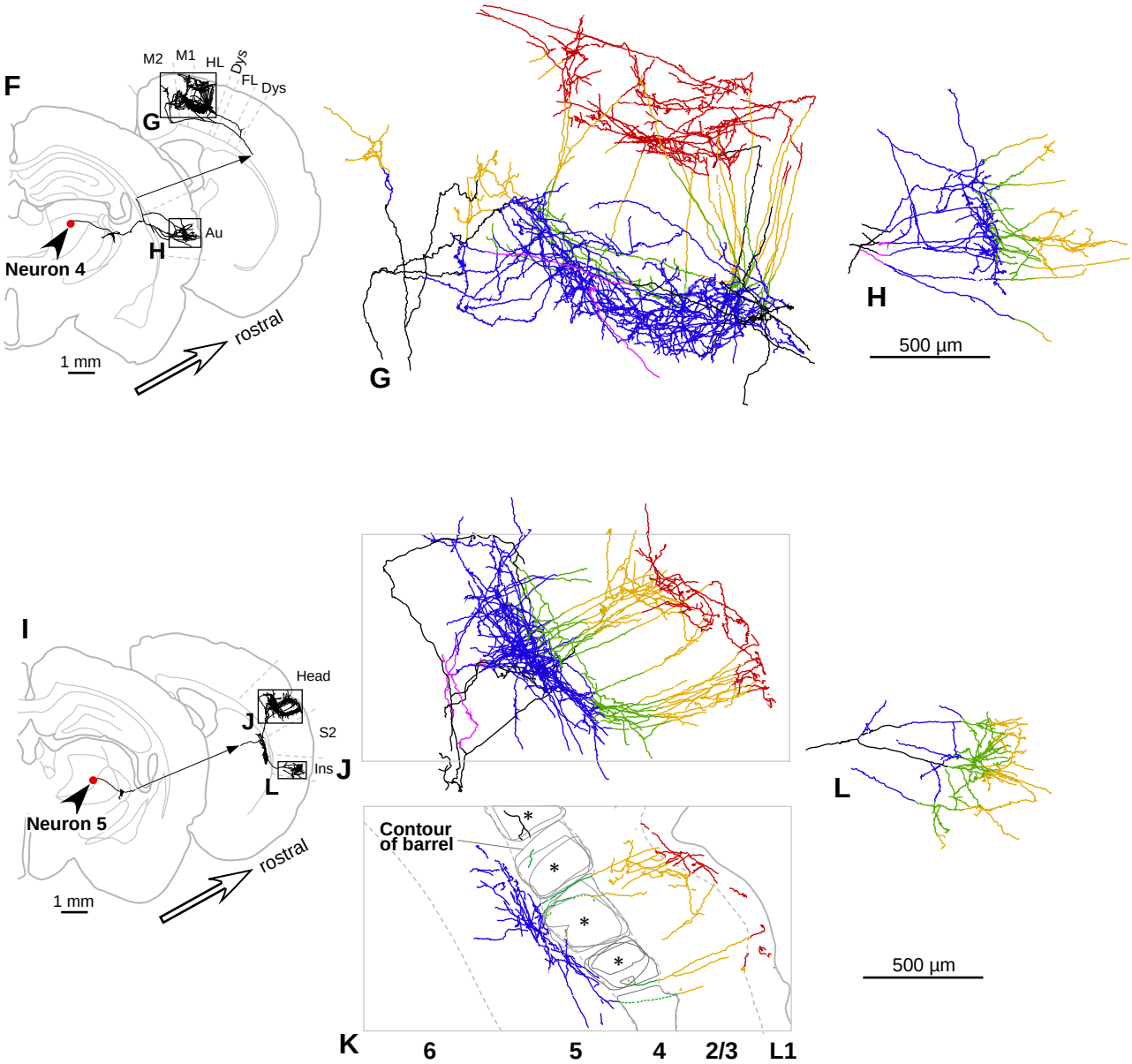

Fig. 5-2 Ohno et al., 169 x 158 mm (double column width) No reduction.

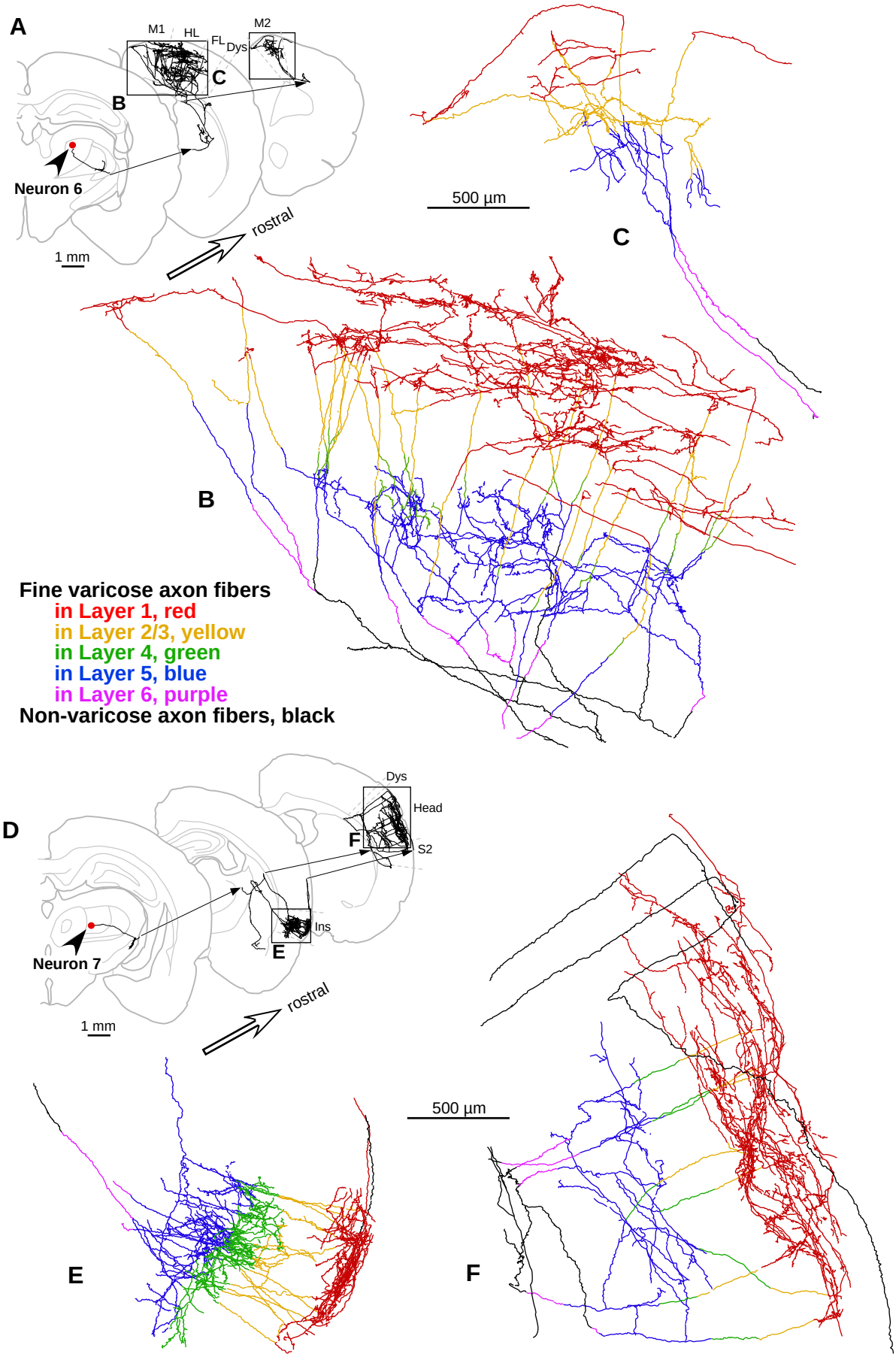

Fig. 6-1 Ohno et al., 157 x 238 mm (double column width) No reduction.

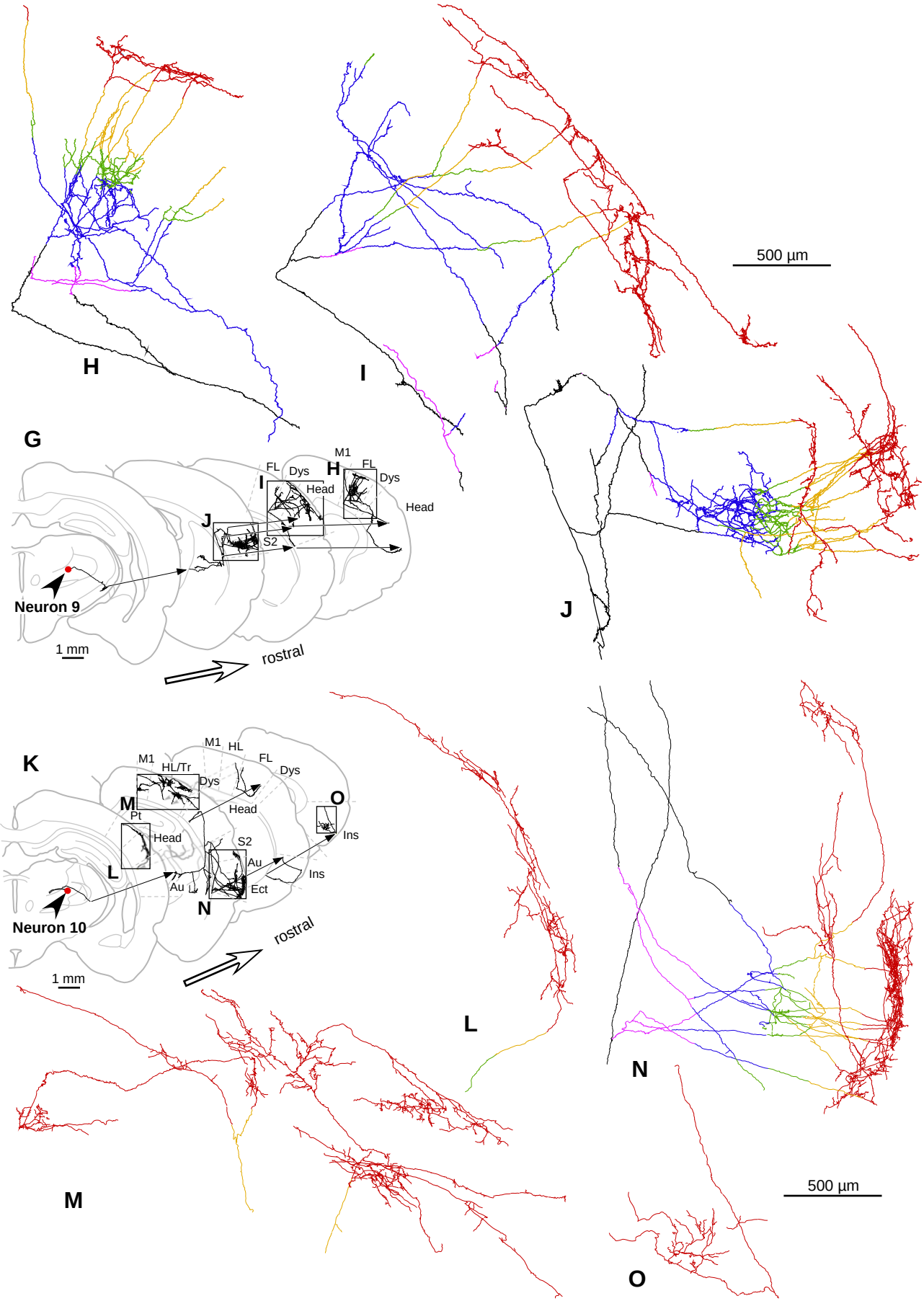

Fig. 6-2 Ohno et al., 169 x 238 mm (double column width) No reduction.

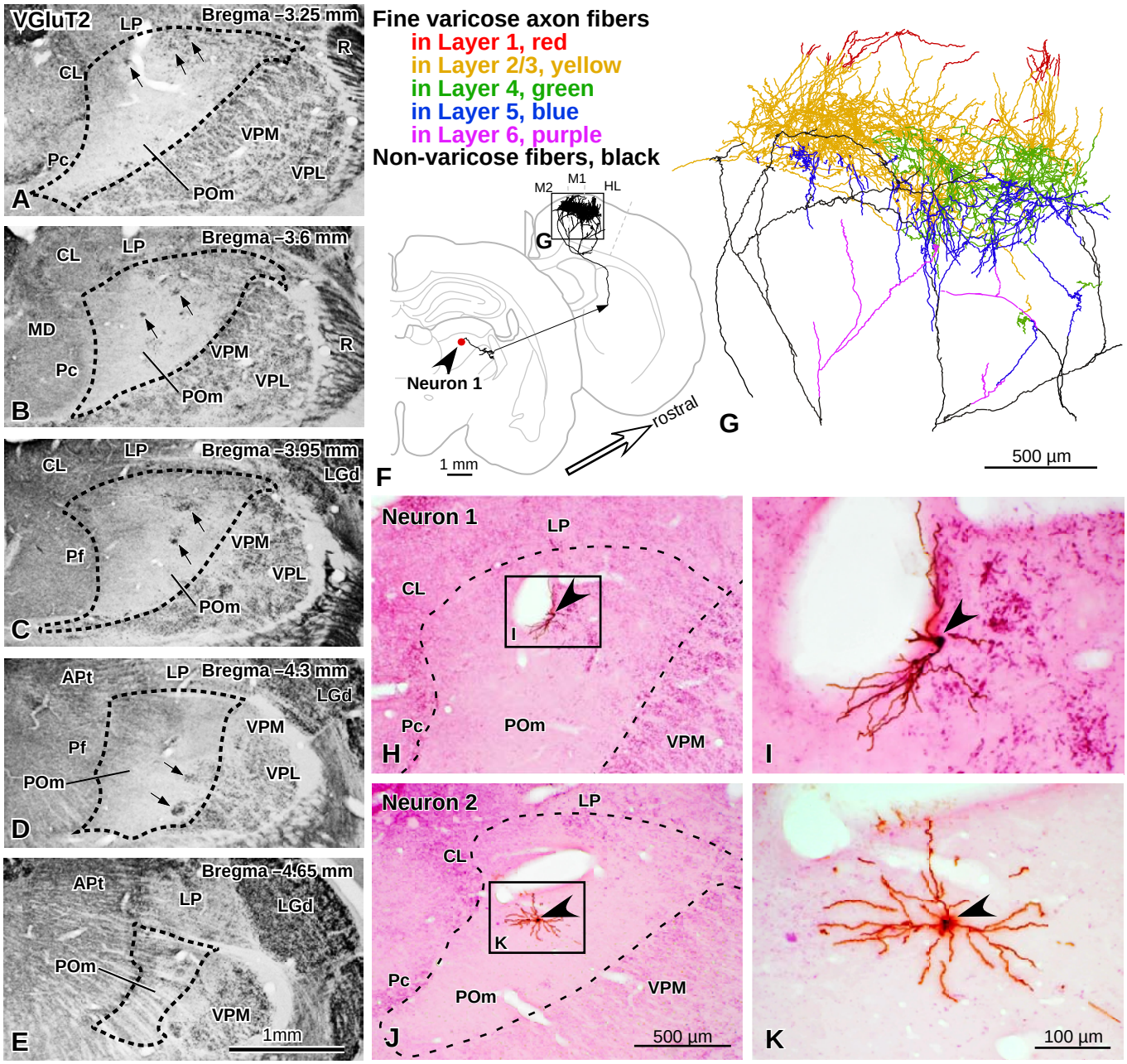

Fig. 7 Ohno et al., 179 x 169 mm (double column width) No reduction.

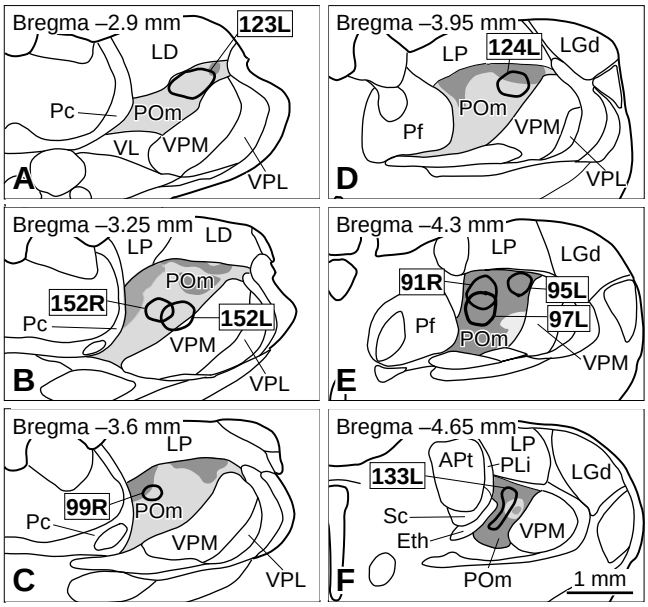

Fig. 8 Ohno et al., No reduction.
85 x 80 mm (single column width)

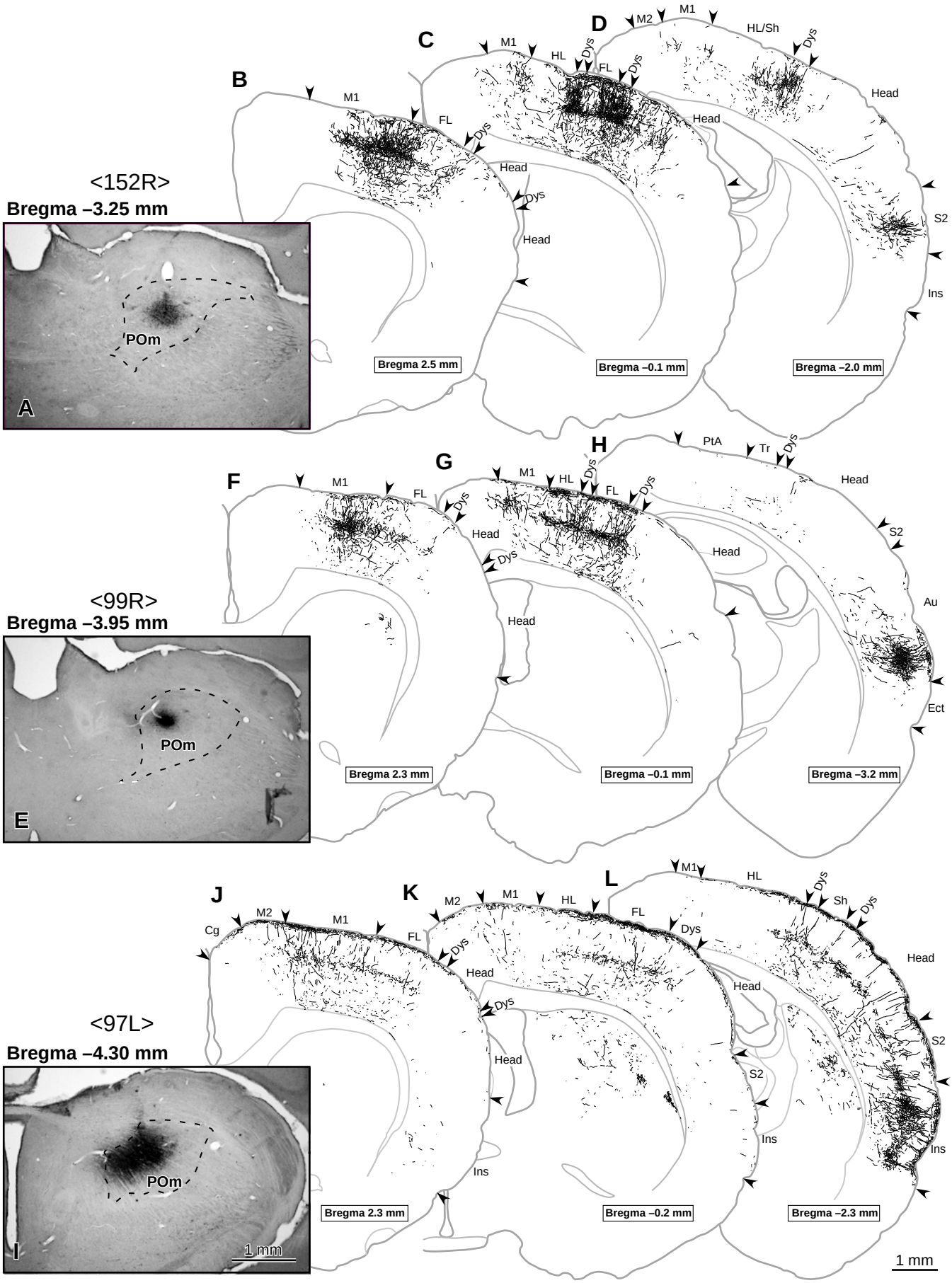

Fig. 9 Ohno et al., 178 x 238 mm (double column width) No reduction.

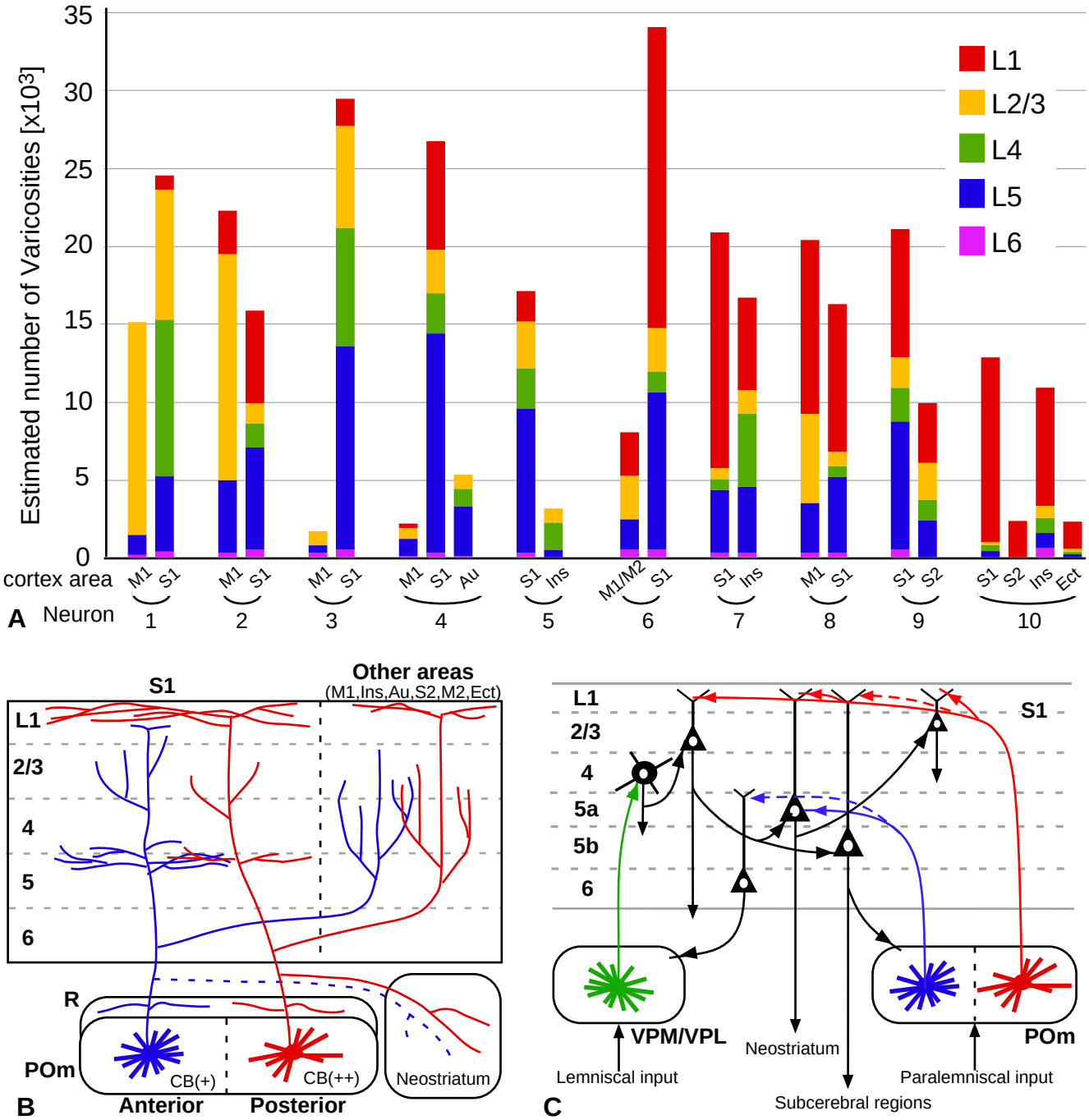

Fig. 10 Ohno et al., 174 x 179 mm (double column width) No reduction.

Supplementary Table 1. The estimated length of varicose axon fibers in each cortical area and layer. The length [μm] of axon fibers was estimated by multiplying the length of varicose axons projected onto a frontal plane by $\pi/2$.

Neuron	cortical areas	cortical layers 1	2/3	4	5	6	total
Anterior POm neurons							
1	S1	4300	59352	52901	26762	3324	146639
	M1	2	85639	0	7556	2555	97834
2	S1	32409	8024	8388	34203	4115	87140
	M1	15733	89716	0	32194	1907	139551
	S2	0	0	0	1002	0	1002
3	S1	9593	44413	40237	70304	3822	168369
	M1	0	5972	0	2577	2039	10588
4	S1	37525	18276	14277	74935	2320	147332
	M1	790	4562	0	6813	374	12539
	Au	0	7305	6323	19750	502	33880
5	S1	10736	20233	13577	49231	2186	95964
	Ins	0	6658	9042	3359	0	19060
Posterior POm neurons							
6	S1	103878	19018	6907	54567	3259	187629
	M1	6802	4657	0	2935	3360	17754
	M2	8371	12307	0	9090	1096	30863
7	S1	81714	4278	3623	21642	2024	113281
	Ins	30749	10982	24322	29133	1994	97181
8	S1	50976	5650	2767	26776	1400	87569
	M1	63723	34201	0	22309	1771	122005
9	S1	44858	13215	10722	43613	4294	116703
	S2	19741	14753	7705	16256	174	58630
10	S1	62807	2405	1063	2641	193	69108
	Ins	40190	5633	5107	6135	4702	61768
	Ect	9350	1117	937	754	0	12159
	M1	5482	0	0	0	0	5482
	S2	12246	0	0	0	0	12246

Supplementary Table 2. The estimated axon length in L4 of granular and dysgranular regions of the S1 cortex.

single-labeled	estimated length of varicose axon fibers in L4 [μm][1]		
POm neuron	entire S1 cortex[2]	granular region	septal/dysgranular region[3]
anterior			
1	52901	52901	0 (0.0%)[3]
2	8388	4693	3695 (44.0)
3	40237	38446	1791 (4.5)
4	14277	10034	4243 (29.7)
5	13577	9761	3816 (28.1)
mean ± S.D.	28576 ±19546	23168±21278	2709 ±1784 (21.3±18.5)
posterior			
6	6907	4313	2595 (37.6)
7	3623	1456	2167 (59.8)
8	2767	2039	727 (26.3)
9	10722	9097	1625 (15.2)
10	1063	443	620 (58.4)
mean ± S.D.	5016 ±3833	3470 ±3451	1547 ±869 (39.5±19.6)
total			
mean ± S.D.	15446 ±17239	13318±17728	2128 ±1458 (30.4±20.4)

1) The length of axon fibers was estimated by multiplying the length projected onto a frontal plane by $\pi/2$.

2) The S1 cortex included HL and FL cortices.

3) The percentage is the relative length within the S1 cortex.

Supplementary Table 3. Inter-bouton interval of cortical axon fibers of POm neurons in each area and layer. The intervals (mean ± S.D. in μm, n = 100) were measured at varicose axon fibers that were anterogradely labeled after injection of PHA-L into the POm (Fig. 8, 9).

cortex \ layer	L1	L2/3	L4	L5	L6
S1	5.42±4.34	6,99±4.35	5.39±4.03	5.39±3.66	8.02±5.70
S2	5.24±3.72	6.95±3.99	5.95±3.74	6.85±5.63	9.22±6.65
M1	5.72±3.81	6.22±3.69	–	6.85±4.71	8.29±5.67
M2	5.48±3.64	6.67±4.60	–	6.39±4.34	8.16±5.81
Insular	5.29±4.17	7.41±5.13	5.29±4.16	7.04±4.17	7.94±5.22
Auditory	5.92±4.29	7.98±5.36	5.81±3.82	6.43±4.86	8.87±6.47
Ectorhinal	5.68±3.75	8.19±5.07	5.83±3.08	6.49±3.75	8.42±6.23

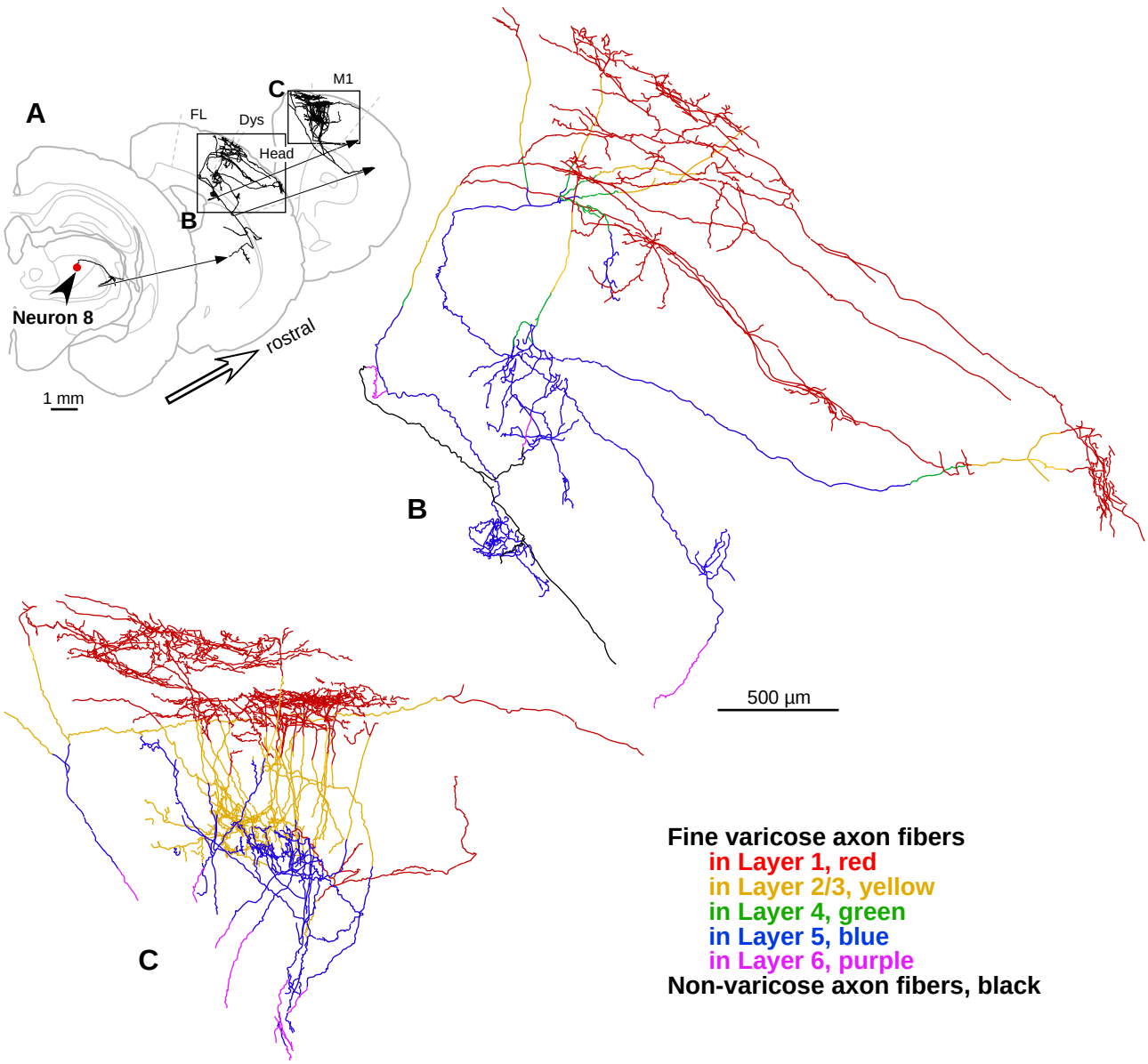

Supplementary Figure 1. The reconstructed axonal arborization of posterior POm neuron 8. For further detail, see the legend of Figure 6.